

Compensator Design By Pole-Zero Adjustment For DC Motor

A Thesis report

submitted towards the partial fulfillment of the

requirements of the degree of

Master of Engineering

in

Electronic Instrumentation and Control Engineering

submitted by

Vivek Sawhney

Roll No-800851027



Under the supervision of

Ms Gagandeep Kaur

Assistant Professor, EIED

Dr. Hardeep Singh

Assistant Professor, ECED

**DEPARTMENT OF ELECTRICAL AND INSTRUMENTATION
ENGINEERING**

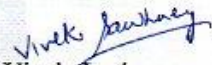
THAPAR UNIVERSITY, PATIALA - 147004

JULY 2010

CERTIFICATE

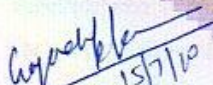
This is to certify that my work presented in this thesis entitled "**Compensator Design By Pole-Zero Adjustment for DC Motor**" in partial fulfillment of the requirement for the award of the degree of **Master of Engineering at Thapar University Patiala**, is an original record under supervision and guidance of **Ms Gagandeep Kaur**, Assistant Professor EIED and **Dr. Hardeep Singh**, Assistant Professor, ECED. The matter embodied in this report has not been submitted anywhere for the award of any other degree of this or any other University.


Date: JULY 15, 2010

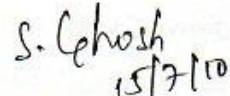

Vivek Sawhney


800851027

It is certified that the above statement made by the student is correct to the best of my knowledge.


Gagandeep Kaur
Assistant Professor, EIED
Supervisor
Thapar University, Patiala


Dr. Hardeep Singh
Assistant Professor, ECED
Co-Supervisor
Thapar University, Patiala


Dr. Smarajit Ghosh
Professor & Head, EIED
Thapar University, Patiala


Dr. R K Sharma
Dean of Academic Affairs
Thapar University, Patiala

ACKNOWLEDGEMENT

The real spirit of achieving a goal is through the way of excellence. I would have never succeeded in completing my task without the cooperation, encouragement and help provided to me by various personalities.

First of all, I render my gratitude to the ALMIGHTY who bestowed self-confidence, ability and strength in me to complete this work. Without his grace this would never come to be today's reality.

With deep sense of gratitude I express my sincere thanks to my esteemed and worthy supervisor **Ms Gagandeep Kaur** in the Department of Electrical and Instrumentation Engineering and Co-supervisor **Dr. Hardeep Singh** in the department of Electronics and Communication Engineering for his valuable guidance in carrying out this work under her effective supervision, encouragement, enlightenment and cooperation. Most of the novel ideas and solutions found in this thesis are the result of our numerous stimulating discussions. Their feedback and editorial comments are also invaluable for writing of this thesis.

I express my deep sense of gratitude towards **Dr. Smarajit Ghosh**, Professor & Head of Electrical and Instrumentation Department who has been a constant source of inspiration for me throughout this work.

I am grateful to **Dr. R.K. Sharma**, Dean of Academic Affair for his constant encouragement that was of great importance in the completion of the thesis.

I extend my thanks to **Dr. K.K. Raina**, Deputy Director, **Dr. Abhijit Mukherjee**, Director Thapar University, for their valuable support that made me consistent performer.

I am also thankful to all the staff members of the Department for their full cooperation and help. My greatest thanks are to all who wished me success especially my parents, my friends whose support and care makes me stay on earth.

Place: Thapar University, Patiala

Date: JULY 15, 2010


Vivek Sawhney

800851027

ABSTRACT

The thesis work mainly relies upon designing of compensator especially lag compensator which can be incorporated into the system in order to improve the response of dc motor without affecting the other parameters. Compensators are specially designed under some design constraints like settling time, rise time, peak overshoot and steady state error. Improving steady state error is the key parameter which has to be taken under consideration. By suitable choice of dc motor constants, transfer functions of open loop and closed loop system are constructed and the corresponding open loop response and closed loop response is observed. The mathematical formulation of transfer function and location of poles and zeros has also been studied. The stability of the system can be analyzed by plotting poles and zeros on the root loci plot. Different compensators are designed by choosing suitable values of poles and zeroes by hit and trial method and the corresponding response curves of different compensators are compared. The closed loop response of dc motor with PID control has also been studied. In order to calculate gain margin and phase margin, bode plot has been plotted. MATLAB is used in order to study different parameters and to plot different response curves.

Organization of the Thesis

1. The first chapter is the review of literature i.e. a summary about the developments in the subject so far.
2. The second chapter gives the basic introduction about DC Motors. It includes the construction, basic principle involved, detailed explanation of working of DC motors, mathematical formulations and applications areas.
3. The third chapter covers the basics concepts about control engineering which are to be used further, to formulate the problem. These concepts are helpful while implementing the results in order to have desired results. This chapter discusses about open loop and closed loop systems, transfer functions, time domain specifications, root loci, bode plot, PID controller etc.
4. The fourth chapter defines the problem upon which the thesis work relies and discusses in detail the algorithm involved.
5. The fifth chapter includes the results obtained after implementation in a particular software and discusses about the results.

TABLE OF CONTENTS

| | |
|--|--------|
| Certificate | i |
| Acknowledgement | ii |
| Abstract | iii |
| Organization of Thesis | iv |
| Table of Contents | v-vii |
| List of figures | viii-x |
| Chapter 1: Literature Review | 1 |
| Chapter 2 : Introduction to DC Motor | |
| 2.1 Overview | 7 |
| 2.2 Construction | 7 |
| 2.3 Principle | 10 |
| 2.4 Single loop motor | 12 |
| 2.4.1 Torque production | 12 |
| 2.4.2 Commutation of single loop motor | 15 |
| 2.5 Modeling an armature controlled DC motor | 17 |
| 2.6 Armature winding | 19 |
| 2.6.1 Lap winding | 19 |
| 2.6.2 Wave winding | 21 |
| 2.7 Slots and coils | 22 |

| | |
|---|----|
| 2.8 Slot pitch | 22 |
| 2.9 Field winding | 22 |
| 2.10 Application areas | 24 |
| Chapter 3 : Control Systems | |
| 3.1 Introduction | 25 |
| 3.2 Open loop and closed loop system | 25 |
| 3.3 Transfer function | 27 |
| 3.4 Poles and zeros of open loop and closed loop system | 27 |
| 3.5 Steady state error | 29 |
| 3.6 State space representation | 30 |
| 3.7 Performance specification of linear system in time domain | 32 |
| 3.8 Bode diagrams | 33 |
| 3.8.1 Stability analysis with Bode Plot | 34 |
| 3.9 Root Locus | 35 |
| 3.9.1 Root Locus drawing rules | 36 |
| 3.9.2 System stability | 37 |
| 3.10 Lag Compensators | 38 |
| 3.10.1 Approaches to system design | 39 |
| 3.10.2 Basic design requirements | 39 |
| 3.10.2.1 Types of compensation | 40 |
| 3.10.3 General rules for lag compensator | 41 |

| | |
|--|----|
| 3.11 PID Control | 42 |
| 3.11.1 Comparison between different types of controllers | 45 |
| Chapter 4 : Problem Definition | |
| 4.1 Problem Definition | 47 |
| 4.2 Implementation | 48 |
| Chapter 5 : Results and Discussions | 53 |
| Conclusions and Future Scope | 67 |
| References | 68 |

LIST OF FIGURES

| S.No. | Figure Number | Figure Name | Page No. |
|-------|---------------|---|----------|
| 1. | Fig 2.1 | DC Motor cutaway view | 7 |
| 2. | Fig 2.2 | DC Motor | 8 |
| 3. | Fig 2.3 | Magnetic force law | 10 |
| 4. | Fig 2.4 | Mathematical formulation of Magnetic force law | 11 |
| 5. | Fig 2.5 | Rotor loop wound around iron core | 12 |
| 6. | Fig 2.6 | A single loop motor | 13 |
| 7. | Fig 2.7 | a) DC motor with a field winding | 14 |
| | | b) Radial magnetic field strength | 14 |
| 8. | Fig 2.8 | a) Position of the rotor when $0 < \theta_r < \pi$ | 15 |
| | | b) Position of the rotor just prior to commutation | 15 |
| | | c) Position of the rotor when $\theta_r = \pi$ | 16 |
| | | d) Rotor loop just after commutation when $\pi < \theta_r < 2\pi$ | 16 |
| 9. | Fig 2.9 | Mathematical model of DC Motor | 17 |
| 10. | Fig 2.10 | a) Lap winding connected to commutator bars | 20 |
| | | b) Circular form | 21 |

| | | | |
|-----|----------|--|----|
| 11. | Fig 2.11 | a) Wave winding connected to commutator bars | 21 |
| | | b) Circular form | 21 |
| | | c) Development form | 12 |
| 12. | Fig 2.12 | Coil sides with armature slots | 22 |
| 13. | Fig 2.13 | Field current connections of dc machines | 23 |
| 14. | Fig 3.1 | Open loop system | 26 |
| 15. | Fig 3.2 | Closed loop system | 26 |
| 16. | Fig 3.3 | Laplace formulation of closed loop system | 26 |
| 17. | Fig 3.4 | Transfer function representation | 27 |
| 18. | Fig 3.5 | Steady state error | 29 |
| 19. | Fig 3.6 | Effect of disturbances on control system | 30 |
| 20. | Fig 3.7 | Time domain specifications | 32 |
| 21. | Fig 3.8 | Cascade compensation | 40 |
| 22. | Fig 3.9 | Feedback compensation | 40 |
| 23. | Fig 3.10 | Feedforward compensation | 41 |
| 23. | Fig 3.11 | Lag compensator design | 41 |
| 24. | Fig 3.12 | PID controller | 42 |
| 25. | Fig 3.13 | Step response of different controllers | 45 |

| | | | |
|-----|----------|---|----|
| 26. | Fig 5.1 | Open loop response without controller | 54 |
| 27. | Fig 5.2 | Closed loop response without controller | 55 |
| 28. | Fig 5.3 | State space representation | 56 |
| 29. | Fig 5.4 | Root locus plot without controller | 57 |
| 30. | Fig 5.5 | Root locus plot with lag compensator | 59 |
| 31. | Fig 5.6 | Open loop response with first lag compensator | 60 |
| 32. | Fig 5.7 | Closed loop response with first lag compensator | 61 |
| 33. | Fig 5.8 | Root locus with final lag compensator | 63 |
| 34. | Fig 5.9 | Closed loop response of dc motor with PID control | 64 |
| 35. | Fig 5.10 | Bode Plot | 65 |
| 36. | Fig 5.11 | Bode plot of closed loop transfer function with final lag compensator | 66 |

CHAPTER 1

LITERATURE REVIEW

Jian Xin Xu has presented a new lead compensator design algorithm by using computation technology which is precise, simple and non-trial-and-error. Hence the new design algorithm overcomes the difficulties in the traditional design. Also two lead compensator design algorithms, either with the maximum phase margin or maximum bandwidth are proposed. For practical applications, the new design based on Bode plots is also exploited. Design examples are provided to facilitate the course teaching and implementation.[11]

Fei-Yue Wang et.al presents the exact and unique solution to the design of phase lead and phase lag compensation when the desired gains in the magnitude and phase are known at a given frequency. It also gives the concise condition for determining the existence of single-stage lead or lag compensation. The phase lead and lag compensation is one of the most commonly used techniques for designing control systems in the frequency domain, especially when the Bode diagram or root locus is used. In most cases, the graphic-based approximation or trial-and-error approach has been used in the design process.[9]

Arjun Godhwani has presented the techniques of feedback control pertinent to understanding power system stabilizer and their tuning. Study of feedback control requires knowledge of various mathematical tools that consist of Laplace transforms, Bode plots, Nyquist plots and Root locus. These tools apply to single-input-single-output systems that are linear and time invariant LTI. The state space approach is used to analyze not only SISO systems but also multiple-input- multiple-output MIMO systems. Some of the systems tend to the nonlinear and are linearized around an operating point for small excursions of the signals before applying these tools. Knowledge of these tools is critical to understanding power system control and stability. Therefore a review of these tools is presented.[15]

Celaleddin Yeroglu presents development of a program in the Matlab for the analysis of fractional order control systems -FOCS. Using this program frequency response plots such as Nyquist plot, Bode plots and Nichols plot can be obtained. Gain and phase margins of FOCS can be estimated and suitable controller can be designed for the related control system.[29]

Marcelo C et.al has proposed that the root-locus method is a well-known and commonly used tool in control system analysis and design. Complementary root locus i.e. plant with negative gain is not as common as root locus plant with positive gain it. This paper shows that complementary root locus can be plotted using only the well-known construction rules to plot root locus. These results present a procedure to avoid problems that appear in root-locus plots for plants with the same number of poles and zeroes.[18]

Tooran Emami et.al has presented a simple, unified design approach for all standard continuous-time and discrete-time classical compensators that is independent of the form of the linear system information. This approach is based on a simple root locus design procedure for a proportional-derivative compensator. From this procedure, design procedures for unified notation lead, proportional-integral -PI, proportional integral-derivative -PID and PI-lead compensator are developed. The delta operator which serves as a link between the continuous-time and discrete-time procedures, offers improved numerical properties to the traditional discrete-time shift operator. With this proposed approach, designers can concentrate on the larger control system design issues, such as compensator selection and closed-loop performance, rather than the intricacies of a particular design procedure.[22]

Thomas J Cavicchi offers visualizations and explanations about phase margin-both its evaluation and its application. The phase-root locus plot reveals the effect of adding phase in the same way that conventional gain root locus shows the effects of adding gain. The phase root locus plot ultimately leads to a definition of phase margin involving phase shifting. This definition of phase margin suggests a simple, effective compensator design method for improving phase margin via phase shifters.[16]

P Dobra et.al discusses about PID control and practical implementations and provides a brief overview on how to tune the parameters of PID controllers. This paper is intended to provide a brief, qualitative overview of how a digital control system is implemented in a familiar analog environment i.e. for DC motor. This paper presents an implementation of PID control algorithm with anti-windup for small DC motor. It also discusses software implementation and presents helpful techniques as well as sample code needed to realize precision control of a motor and also given a brief overview of the control of a DC motor using pulse width modulation.[30]

Yeung Kai Shing et.al proposed that a single universal design chart can be generated for all the various types of conventional compensators. Recently design charts were given for various conventional compensators. In particular a design chart was developed for the phase-lead-lag compensator to eliminate the trial-and error nature of the design. This chart allows compensator parameters to be determined readily and is applicable to the design of both continuous-time and discrete-time compensators. A detailed example is given to illustrate the use of the chart. This universal chart may be computerized for ease of design.[5]

Miroslav Markovic et.al presents an application of the Matlab optimization algorithms to a slotless brushless DC motor design with seven design parameters. The tested algorithms are: classical or gradient-based, direct-search and genetic. As a conclusion, the direct-search algorithm is not suitable for this application, as it is highly dependent on the initial values. The classical or genetic algorithms are suitable to apply, but within loops. The best results are produced by the sequence genetic-classical algorithms.[23]

N Bianchi et.al presents the design of a 1kW permanent magnet brushless motor operating at 20-40 rpm. The design procedure involves parametrical researches of the most convenient motor configuration through a coupled thermal and electromagnetic analysis. The preliminary design is based on the solution of Maxwell's equations and is followed by a finite element analysis. A slotted and a slotless motor configurations have

been taken into account with different permanent magnet materials for an overall comparison of the motor performance.[17]

Zhang Dailin et.al has designed a position angle error compensator to compensate the position angles detected by linear encoders. The position angle is very important in the current control of permanent-magnet linear motors and its error affects the control precision of currents. The position angle is generally not accurately detected because of faults in motor making, pulse loss of linear encoders and so on. In order to control the currents of permanent-magnet linear motors precisely, a compensation scheme of position angle errors is proposed based on the mathematical relation between position angle errors and currents. Furthermore a filter and a class of iteration learning algorithm are proposed to avoid the errors produced by detected phase currents and phase voltages. Simulation results show that position angle errors of PMLMs are fully compensated. Using the designed position angle error compensator, currents can be controlled in a more precise manner.[24]

Michael Ruderman et.al describes a novel compensation technique based on disturbance observation and a self-tuning feed-forward compensation algorithm. The DC motor is modeled as a linear system augmented by the nonlinear Coulomb friction and is experimentally identified from a set of the system responses. The disturbance harmonics are detected by means of the fast Fourier transformation and analytically described by a spatial Fourier transform with respect to the angular position of the rotor. The online algorithm tunes the parameters of the feed-forward compensator using the recursive estimation technique. The proposed self-tuning compensator is experimentally verified as part of an open control loop at different level of the rotational velocity and system load.[28]

Yang Song has proposed a new repetitive adaptive compensation scheme for the dynamic friction and periodic ripple moment in a DC motor system. The paper's contribution is to add repetitive control scheme into the adaptive-based compensation scheme. A Luge dynamic friction model with non-uniformly variational parameters is used in the motor

system. The compensation algorithm consists of a PD component, an adaptive component and a repetitive component. The adaptive component is to estimate and compensate for the unknown model parameters, moreover the induced repetitive controller is motivated by the attempt to improve the system motion trajectory tracking performance. The system stability and the uniformly ultimately position tracking performance are guaranteed by utilizing Lyapunov method. Finally computer simulations verify the effectiveness of the proposed scheme for the high precision servo system.[20]

Jonathan Scott et.al has presented a method for speed control of brushed dc motors. It is particularly applicable to motors with armatures of less than 1cm^3 . Motors with very small armatures are difficult to control using the pulse width-modulation approach and are apt to overheat if driven. The technique regulates speed via the back electromotive force but does not require current discontinuous drives. Armature heating in small motors under pulse width-modulation drive is explained and quantified. The method is verified through simulation and measurement. Control is improved and armature losses are minimized. The method can expect to find application in miniature mechatronic equipment.[31]

Hwa R Hur et.al has designed a predictive controller based upon stochastic methods to compensate the time-delay on a system that inherently has time-delay caused by the spatial separation between controllers and actuators. The predictive controller estimates current outputs using a linear prediction function and a probability function in terms of previous outputs and minimizes the malicious phenomena caused by time-delay in the precise control systems. To demonstrate effectiveness of this control methodology, this algorithm is applied to controlling of a remote operated DC servomotor. The experimental results show that this predictive controller is superior to the conventional PID controller in terms of convergence characteristics and also show that this controller expands the maximum allowable time-delay for a system. Since the proposed predictor does not require a specific model for the plant -- it requires only stochastic information on the outputs, it can be applied to the control of general non-linear systems.[3]

J X Shen et.al has proposed an idea that a PM brushless DC motor can be sensorlessly controlled using phase voltage or terminal voltage. But such control might cause detection error of the rotor position. This paper will compute and analyze the detection error and the motor commutation angle and present an error compensation circuit to make the motor commutated normally. Experimental results will be included to verify the computation equations and the compensation circuit.[4]

Thanh H Tran et.al presents a new method for elimination of the step response overshoot in a conventional PID-controlled system and enhancement of its robustness by cascading a sliding mode controller in the outer loop. The idea is first to use the cascade control principle to model the under-damped system under PID control with a second-order system. Then by making use of the sliding mode control outer loop a robust, reduced-order response can be obtained to suppress the control overshoot. The proposed approach can also deal with time delay systems. Its validity is verified through simulation for some dynamic systems subject to highly nonlinear uncertainties, where overshoot remains an issue.[25]

Jiraphon Srisertpol et.al demonstrated a method for estimating the variable torque of DC motors by using a method called “adaptive compensation”. The results of the study can be used to improve and develop the performance of DC motor control systems. DC motor drives are widely used in industry for drive systems such as conveyors and hydraulic servo motors. The performances of DC motor control systems are reduced by the effect of DC motor variable torque. The control system of a DC motor will increase the electric current in a DC motor to maintain a desirable speed when the DC motor receives the variable torque or disturbance torque. Generally, the variable torque of a DC motor is difficult to measure in practice but it can be estimated.[32]

CHAPTER 2

INTRODUCTION TO DC MOTOR

2.1 Overview

The direct current motor is one of the first machines devised to convert electrical power into mechanical power. Direct-current motors as the name implies use direct-unidirectional current. DC motors are used in special applications where high torque starting or smooth acceleration over a broad speed range is required. DC motors have the potential for very high torque capabilities, are easy to miniaturize and can be throttled by adjusting their supply voltage. DC motors are not only the simplest, but the oldest electric motors.

2.2 Construction

A typical DC generator or motor usually consists of: an armature core, an air gap, poles and a yoke which form the magnetic circuit; an armature winding, a field winding brushes and a commutator which form the electric circuit and a frame, end bells, bearings, brush supports and a shaft which provide the mechanical support.

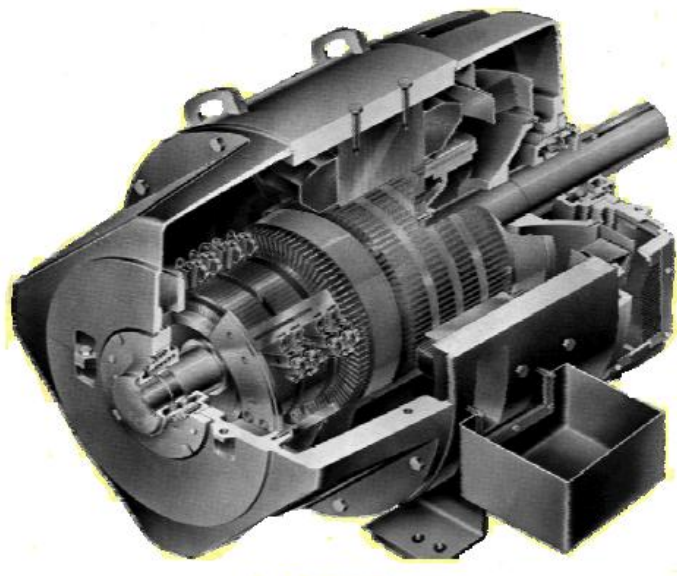


Fig 2.1 DC motor-cutaway view

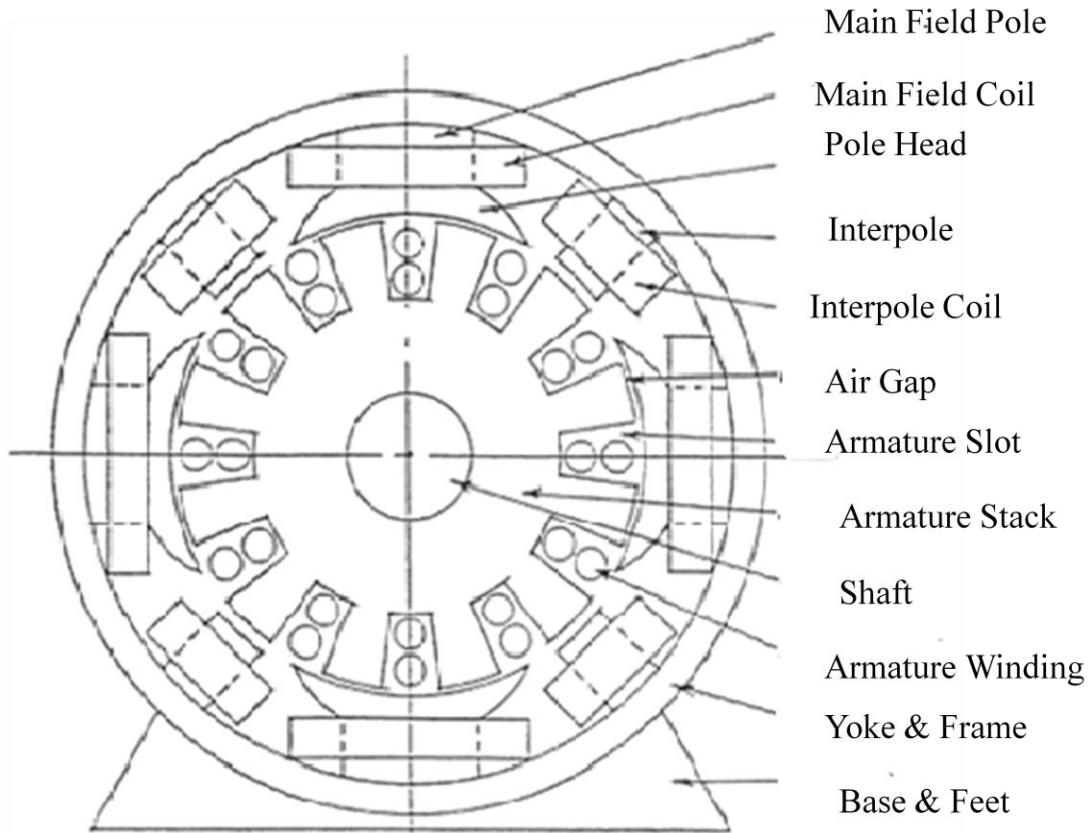


Fig 2.2 DC motor

(i) Armature Stack

The armature stack is made up from thin magnetic steel laminations stamped from sheet steel with a blanking die. Slots are punched in the lamination with a slot die. Sometimes these two operations are done as one. The laminations are welded, riveted, bolted or bonded together.

(ii) Armature Winding

The armature winding is the winding which fits in the armature slots and is connected to the commutator. It either generates or receives the voltage depending on whether the unit is a generator or motor. The armature winding usually consists of copper wire either round or rectangular and is insulated from the armature stack.

(iii)Field Poles

The pole cores can be made from solid steel castings or from laminations. At the air gap the pole usually fans out into a pole head or pole shoe. This is done to reduce the reluctance of the air gap. Normally the field coils are formed and placed on the pole cores and then the whole assembly is mounted to the yoke.

(iv)Field Coils

The field coils are those windings which are located on the poles and set up the magnetic fields in the machine. Field coils consist of copper wire which is insulated from the poles. The field coils may be either shunt windings i.e. connected in parallel with the armature winding or series windings i.e. connected in series with the armature winding or a combination of both.

(v)Yoke

The yoke is a circular steel ring which supports the field, poles mechanically and provides the necessary magnetic path between the pole. The yoke can be solid or laminated. In many DC machines, the yoke also serves as the frame.

(vi)Commutator

The commutator is the mechanical rectifier which changes the AC voltage of the rotating conductors to DC voltage. It consists of a number of segments normally equal to the number of slots. The segments or commutator bars are made of silver bearing copper and are separated from each other by mica insulation.

(vii)Brushes and Brush Holder

Brushes conduct the current from the commutator to the external circuit. There are many types of brushes. A brush holder is usually a metal box that is rectangular in shape. The brush holder has a spring that holds the brush in contact with the commutator. Each brush has a flexible copper shunt which extends to the lead wires. Generally the entire brush assembly is insulated from the frame and is made movable as a unit about the commutator to allow for adjustment.

(viii)Interpoles

Interpoles are similar to the main field poles and located on the yoke between the main field poles. They have windings in series with the armature winding. Interpoles have the

function of reducing the armature reaction effect in the commutating zone. They eliminate the need to shift the brush assembly.

(viii)Frame, End Bells, Shaft, Bearings

The frame and end bells are usually steel, aluminum or magnesium castings used to enclose and support the basic machine parts. The armature is mounted on a steel shaft, which is supported between two bearings. The bearings are either sleeve, ball or roller type. They are normally lubricated by grease or oil.

(ix)Back End, Front End

The load end of the motor is the back end. The opposite load end most often the commutator end is the front end of the motor.

2.3 Principle

Motors work on the basic principle that magnetic fields produce forces on wires carrying a current. If one places a current carrying wire between the poles of a magnet as in figure 2.3, a force is exerted on the wire. Experimentally the magnitude of this force is proportional to both the amount of current in the wire and to the length of the wire that is between the poles of the magnet. That is F_{mag} is proportional to li . The direction of the magnetic field B at any point is determined by a small compass needle. This direction is indicated by arrows in between the north and south poles in figure 2.3.

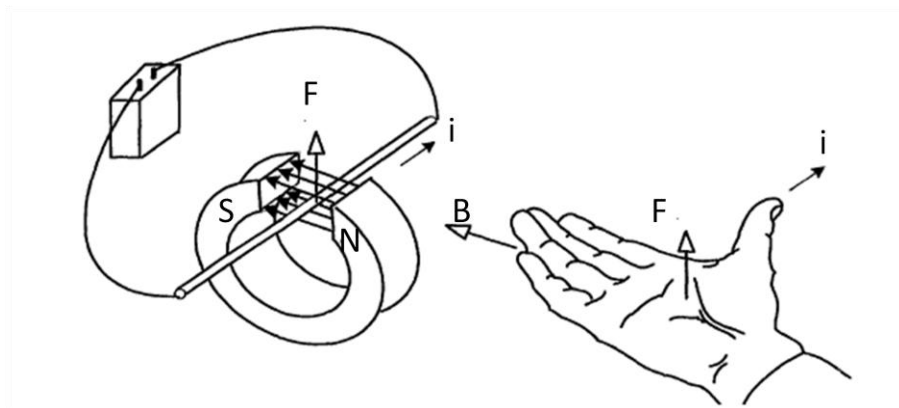


Fig 2.3 Magnetic force law

With the direction of B perpendicular to the wire, the magnitude of the magnetic induction field B is defined as

$$B = |\vec{B}| = \frac{F_{\text{mag}}}{li}$$

Where F_{mag} is the magnetic force, i is the current and l is the length of wire perpendicular to the magnetic field carrying the current. B is the proportionality constant so that $F_{\text{mag}} = ilB$. As illustrated in figure 2.3, the direction of the force can be determined using the right-hand rule. Using right hand, point the fingers in the direction of the magnetic field and thumb in the direction of the current. Then the direction of the force is out of the palm.

Further experiments show that if the wire is parallel to the B field rather than perpendicular as in figure 2.3, then no force is exerted on the wire. If the wire is at some angle θ with respect to B as in figure 2.4, then the force is proportional to the component of B perpendicular to the wire that is it is proportional to $B_{\perp} = B\sin(\theta)$. This is summarized in the magnetic force law: Let l denote a vector whose magnitude is the length l of the wire in the magnetic field and whose direction is defined as the positive direction of current in the bar; then the magnetic force on the bar of length l carrying the current i is given by

$$F_{\text{mag}} = il * B$$

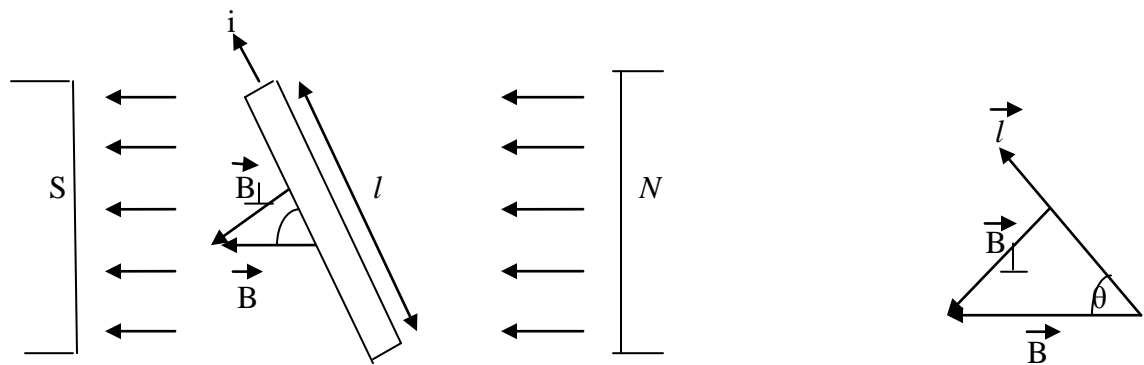


Fig 2.4 Magnetic force law -Mathematical formulation

2.4 Single-Loop Motor

As a first step to modeling a DC motor, a simplistic single-loop motor is considered. It is first shown how torque is produced and then how the current in the single loop can be reversed or commutated every half turn to keep the torque constant.

2.4.1 Torque Production

Consider the magnetic system in figure 2.5 where a cylindrical core is cut out of a block of a permanent magnet and replaced with a soft iron core.

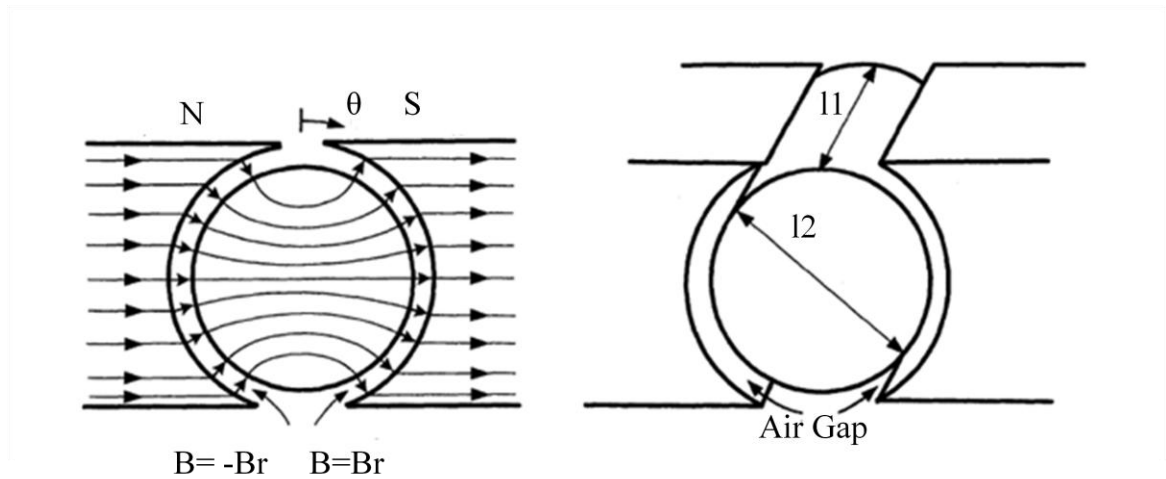


Fig 2.5 Rotor loop wound around iron core

A mathematical description of the magnetic field in the air gap due to the permanent magnet is simply

$$B = \begin{cases} Br & \text{for } 0 < \theta < \pi \\ -Br & \text{for } \pi < \theta < 2\pi \end{cases}$$

where $B > 0$ is the magnitude or strength of the magnetic field and θ is an arbitrary location in the air gap.

Figure 2.5 shows a rotor loop wound around the iron core. The length of the rotor is l_1 and its diameter is l_2 . The torque on this rotor loop is calculated by considering the magnetic forces on sides a and a' of the loop. On the other two sides of the loop i.e. the front and back sides, the magnetic field has negligible strength so that no significant force

is produced on these sides. As illustrated in figure 2.6(b), the rotor angular position is taken to be the angle θ_R from the vertical to side a of the rotor loop

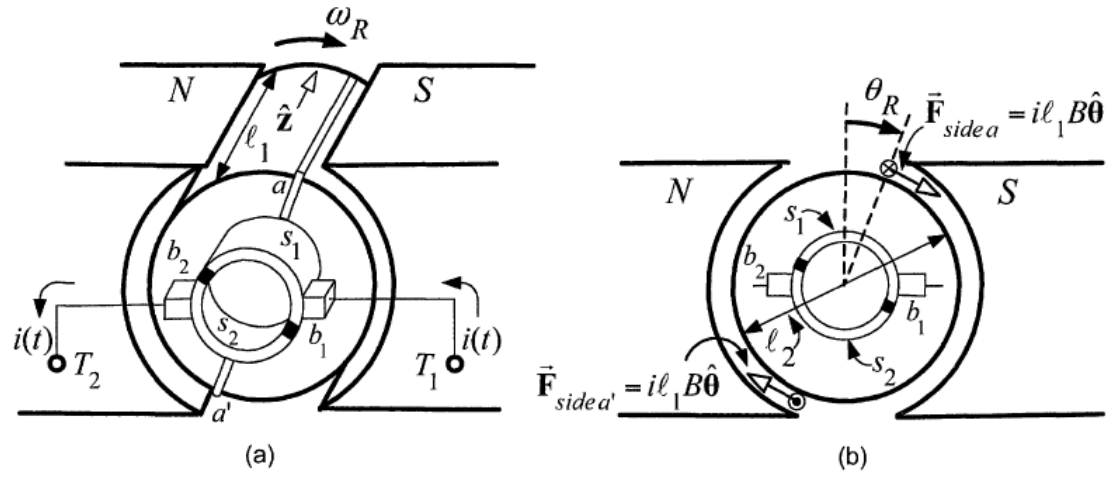


Fig 2.6 A single-loop motor

Referring back to figure 2.5 for $i > 0$, the current in side a of the loop is going into the page and then comes out of the page on side a' . Thus on side a , $l = l_1 \hat{z}$ and the magnetic force $F_{side a}$ on side a

$$\begin{aligned} F &= i\vec{l} * \vec{B} \\ &= i(l_1 \hat{z}) * (B \hat{r}) \\ &= il_1 B \hat{\theta} \end{aligned}$$

which is tangential to the motion as shown in figure 2.6(b). The resulting torque is

$$\begin{aligned} \vec{\tau}_{side a} &= \left(\frac{l_2}{2}\right) \hat{r} + \vec{F}_{side a} \\ &= \left(\frac{l_2}{2}\right) il_1 B \hat{r} * \hat{\theta} \\ &= \left(\frac{l_2}{2}\right) il_1 B \hat{z} \end{aligned}$$

Similarly the magnetic force on side a' of the rotor loop is

$$\vec{F}_{side a'} = i\vec{l} * \vec{B}$$

$$= i(-l_1 \hat{z}) * (-B \hat{r})$$

$$= il_1 B \hat{\theta}$$

so that the corresponding torque is

$$\vec{\tau}_{side a} = \left(\frac{l_2}{2}\right) \hat{r} * \vec{F}_{side a}$$

$$= \left(\frac{l_2}{2}\right) il_1 B \hat{r} * \hat{\theta}$$

$$= (l_2/2) il_1 B \hat{z}$$

The total torque on the rotor loop is then

$$\tau_m = \vec{\tau}_{side a} + \vec{\tau}_{side a'}$$

$$= 2 \left(\frac{l_2}{2}\right) il_1 B \hat{z}$$

$$= l_1 l_2 B i \hat{z}$$

The torque points along the z axis, which is the axis of rotation.

In order to increase the strength of the magnetic field in the air gap, the permanent magnet can be replaced with a soft iron material with wire wound around the periphery of the magnetic material as shown in figure 2.7(a). This winding is referred to as the field winding and the current it carries is called the field current.

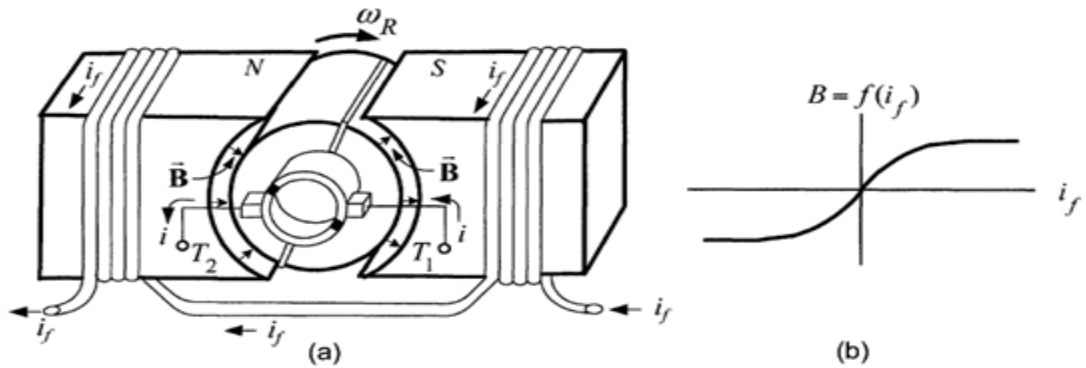


Fig 2.7 (a) DC motor with a field winding (b) Radial magnetic field

strength in the air gap produced by field current

2.4.2 Commutation of the Single-Loop Motor

The process of changing the direction of the current is referred to as commutation and is done at $\theta_R = 0$ and $\theta_R = \pi$ through the use of the slip rings s_1, s_2 and brushes b_1, b_2 drawn in figure 2.8. The slip rings are rigidly attached to the loop and thus rotate with it. The brushes are fixed in space with the slip rings making a sliding electrical contact with the brushes as the loop rotates.

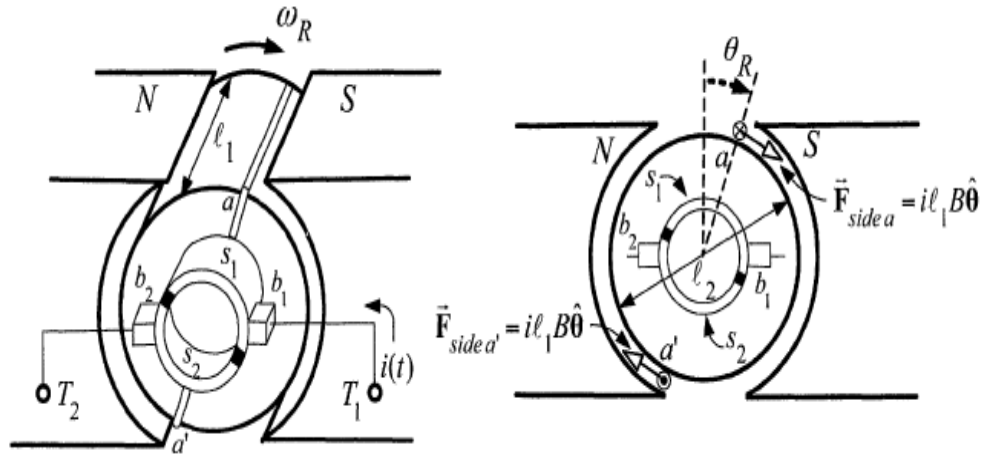


Fig 2.8(a) Position of the rotor when $0 < \theta_R < \pi$

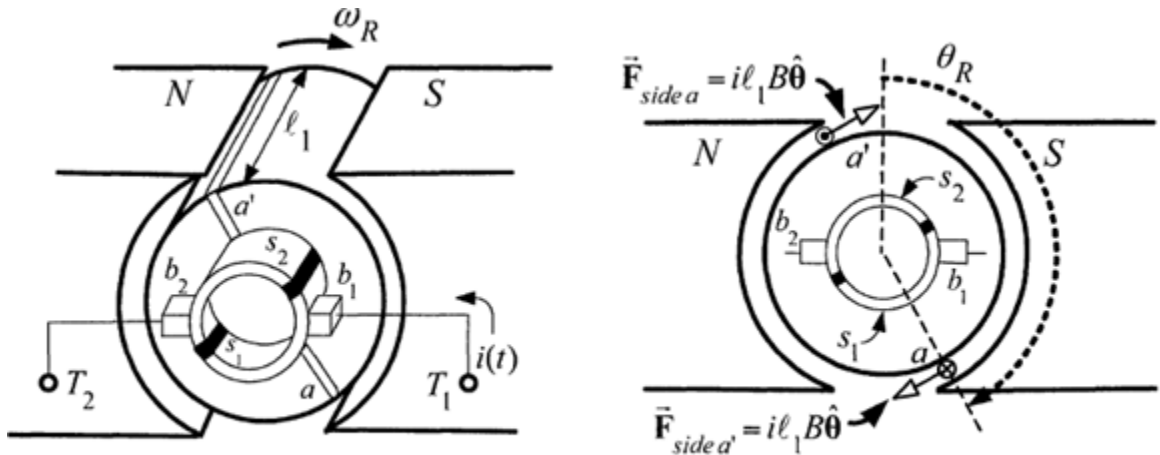


Fig 2.8(b) Rotor loop just prior to commutation where $0 < \theta_R < \pi$

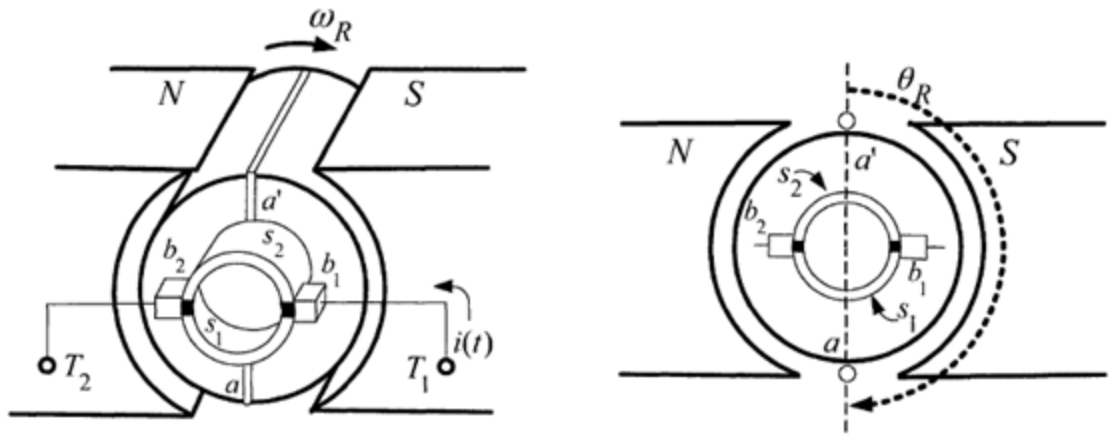


Fig 2.8(c) The ends of rotor loop are shorted when $\theta_R = \pi$

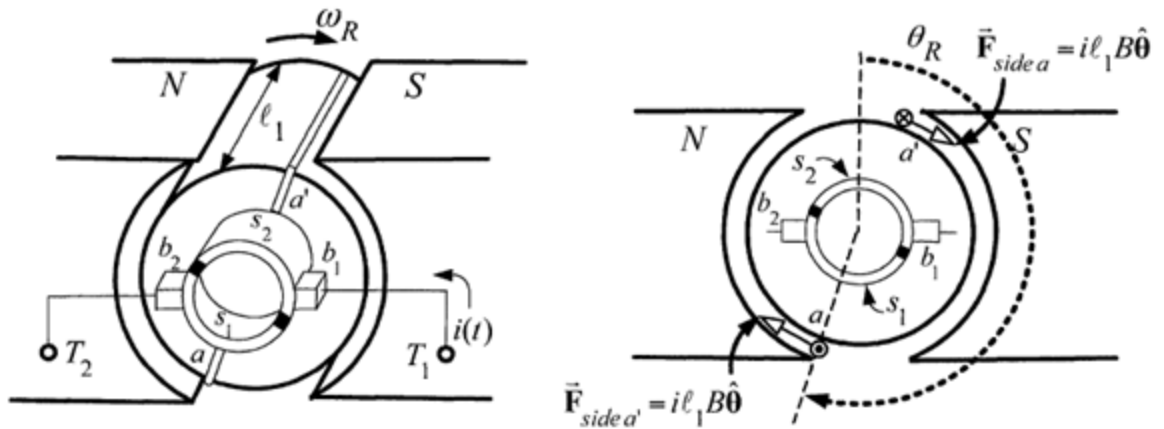


Fig 2.8 (d) Rotor loop just after commutation where $\pi < \theta_r < 2\pi$

To see how the commutation of the current is accomplished using the brushes and slip rings, consider the sequence of figures 2.8(a)-(d). As shown in figure 2.8(a) the current goes through brush b_1 into the slip ring s_1 . From there, it travels down i.e. into the page, in regard to side a of the loop, comes back up side a' out of the page into the slip ring s_2 and finally comes out the brush b_2 . Figure 2.8(b) shows the rotor loop just before commutation where the same explanation holds as in figure 2.8(a). Figure 2.8(c) shows that when $\theta_R = \pi$, the slip rings at the ends of the loop are shorted together by the brushes

forcing the current in the loop to drop to zero. Subsequently as shown in figure 2.8(d) with $\pi < \theta_R < 2\pi$, the current is now going through brush b_1 into slip ring s_2 . From there the current travels down into the page side a' of the loop and comes back up out of the page side a . In other words the current has reversed its direction in the loop from 2.8(a) and 2.8(b). As a result of the brushes and slip rings, the current direction in the loop is reversed every half-turn.

2.5 Modeling an Armature Controlled DC Motor

Let us mathematically model the transfer function of an armature controlled DC motor. The electrical equivalent diagram of an armature controlled DC motor is given in the figure below.

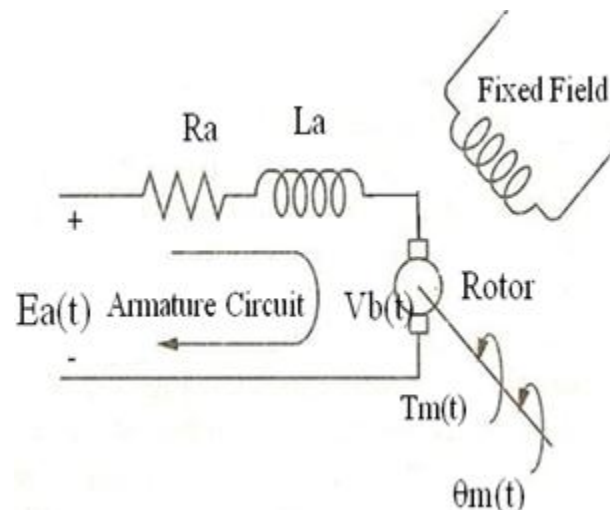


Fig 2.9 Mathematical model of DC motor

R_a is the equivalent armature resistance

L_a is the self inductance of the armature

e_a is the excitation voltage

i_a is the current flowing through the armature

v_b is the back e.m.f generated in the armature circuit

T_m is the total electromagnetic torque produced by the motor

q_m is the angular displacement of the rotor shaft

J_m is the combined equivalent moment of inertia of motor and load w r t motor shaft

B_m is the combined equivalent viscous friction coefficient motor and load w.r.t motor shaft

Writing the KVL equation for the armature circuit we get

$$R_a i_a(t) + L_a \frac{di_a(t)}{dt} + v_b(t) = e_a(t) \quad (1)$$

The back e.m.f generated in the armature circuit is proportional to the angular velocity of the shaft since the field current is constant and hence the flux is constant.

We can express the back e.m.f as

$$v_b(t) = K_b \frac{d\theta_m(t)}{dt} \quad (2)$$

Where K_b is the back e.m.f constant.

The torque developed by the motor is proportional to the armature current. Thus we have

$$\tau_m(t) = K_t i_a(t) \quad (3)$$

Transforming the above three equations to the frequency domain by taking the Laplace transform and substituting for current from equation (3) we get

$$\frac{(R_a + L_a s)T_m(s)}{K_t} + K_b s \theta_m(s) = E_a(s) \quad (4)$$

Now the torque in terms of the angular position is given by the equation

$$\tau_m(s) = (J_m s^2 + B_m s)\theta_m(s) \quad (5)$$

Now substituting equation(5) in equation(4) we get

$$\frac{(R_a + L_a s) (J_m s^2 + B_m s)}{K_t} \theta_m(s) + K_b s \theta_m(s) = E_a(s) \quad (6)$$

Here L_a represents the leakage inductance corresponding to the flux not utilized for generating the torque and it is a very small quantity and can be neglected. Hence we can rearrange equation (6) in the transfer function form as

$$\frac{\theta_m(s)}{E_a(s)} = \frac{K_t}{R_a J_m s^2 + (R_a B_m + K_b K_t) s} \quad (7)$$

. This can be further simplified as

$$\begin{aligned} \frac{\theta_m(s)}{E_a(s)} &= \frac{K_t}{\{R_a J_m s + (R_a B_m + K_b K_t)\} s} \\ &= \frac{K_t / (R_a B_m + K_b K_t)}{s(1 + s \left(\frac{R_a J_m}{R_a B_m + K_b K_t} \right))} \\ \frac{\theta_m(s)}{E_a(s)} &= \frac{K_m}{s(1 + s T_m)} \end{aligned} \quad (8)$$

Where K_m is the motor gain constant defined as $K_m = \frac{K_t}{R_a B_m + K_b K_t}$

And T_m is the motor time constant defined as $T_m = \frac{R_a J_m}{R_a B_m + K_b K_t}$

2.6 Armature Windings

2.6.1 Lap Winding

When the end connections of the coils are brought to adjacent bars as shown in figure 2.10, a lap or parallel winding is formed. In this type of winding, there are as many paths through the armature as there are poles on the machine. To have a full advantage of this winding, the number of brushes should be approximately same as the number of poles, alternate brushes being positive and negative. Any winding can be illustrated in one of two forms, the circular form or the development form. A simplex lap winding is shown in figure as a circular form and development form. In circular form, the flux cutting portions of the conductors are shown as straight lines radiating from the center and are numbered

for convenience in connecting them to the commutator which is in the center of the diagram. The outermost connecting lines represent the end connections on the back of the armature and the inner connecting lines represent the connections on the front or commutator end of the armature. The development form of winding represents the armature as split open and rolled out flat. The lap winding is best suited for low voltage, high current ratings due to large number of parallel paths.

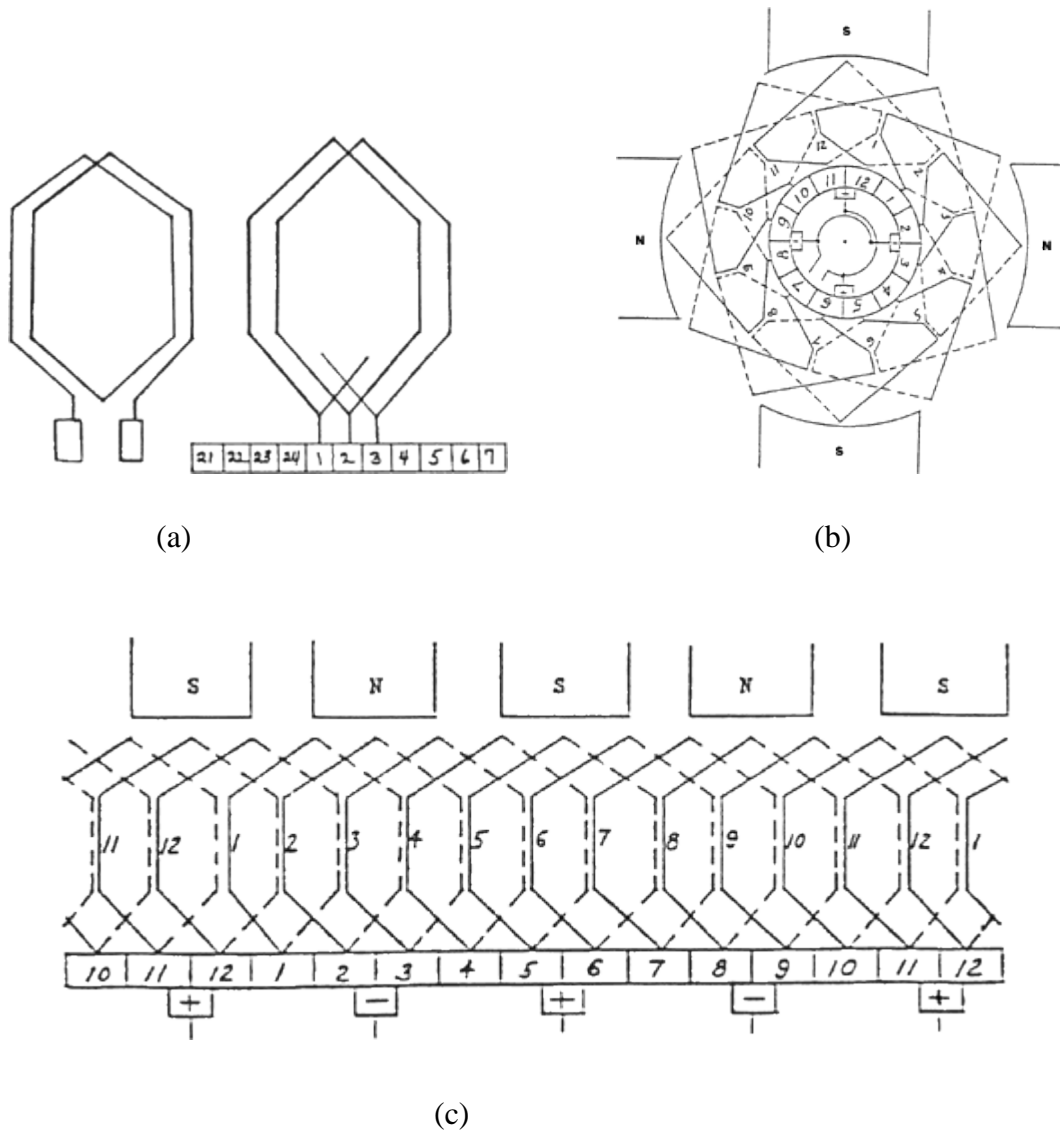


Fig 2.10 (a) Lap winding connected to commutator bars

(b) Circular Form (c) Development Form

2.6.2 Wave Winding

When the end connections of the coils are spread apart as shown in figure 2.11 a wave or series winding is formed. In a wave winding there are only two paths regardless of the number of poles. This type of winding requires only two brushes but can use as many brushes as poles. The simplex wave winding in circular form and development form shows that the connections to the armature do not lap back towards the coil but progress forward. The coil voltages are cumulative but in order to trace the path between the positive and negative brush, it is necessary to travel several times around the armature and to traverse half the total winding. The wave winding is best suited for high voltage low current ratings since it has only two paths.

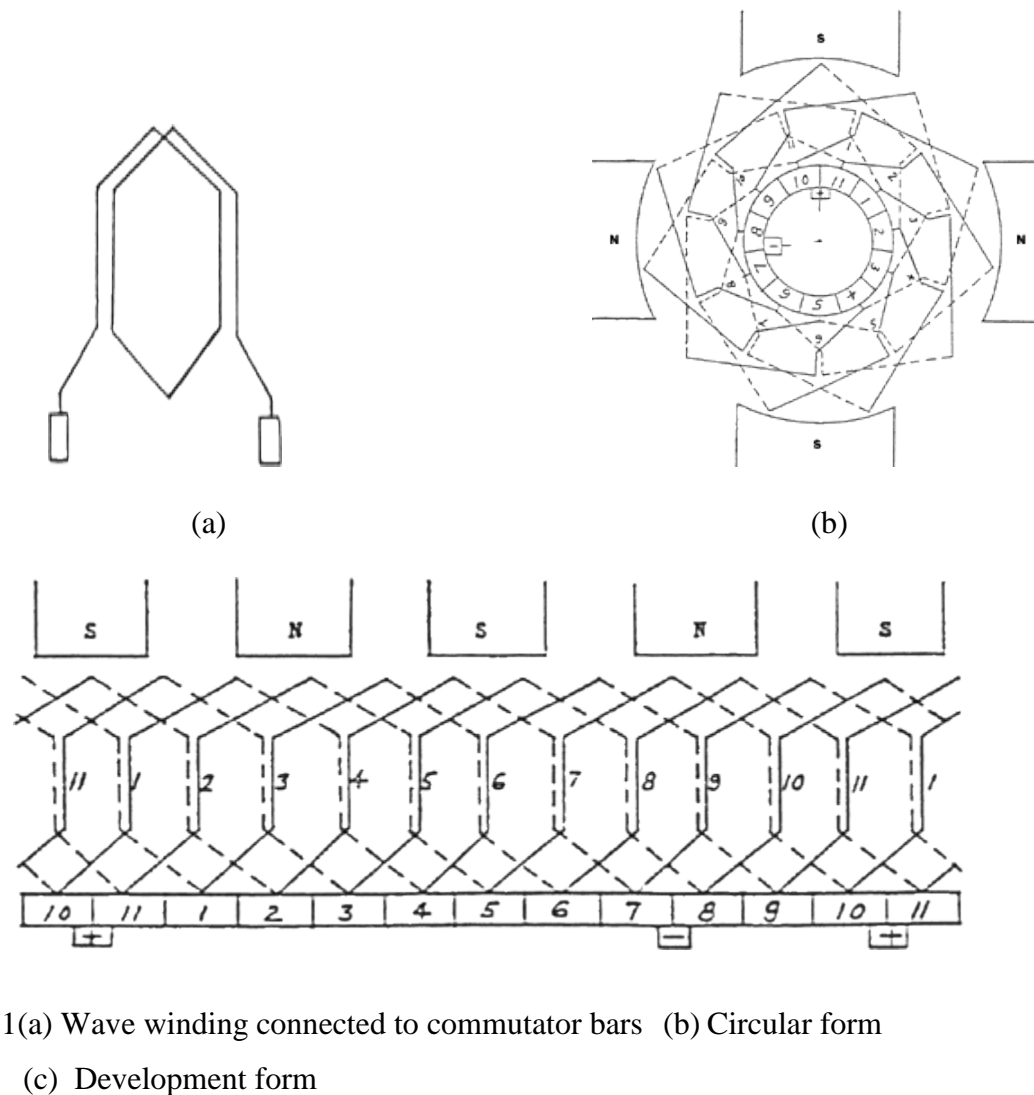


Fig 2.11(a) Wave winding connected to commutator bars (b) Circular form
(c) Development form

2.7 Slots and Coils

The number and size of slots depend upon the generator or motor requirements. The slot should be so chosen that it can hold the suitable number of conductors. In a simple winding the number of coils are approximately same as the number of slots. Therefore each slot contains two coil sides, one side of each coil being at the top of a slot and the other at the bottom of a slot. Each coil consist of one or more turns depending on the applied or generated voltage of the unit. A typical arrangement of coil sides and slots is shown in figure 2.12. Solid lines represent the front end connections to the commutator and dotted lines represent the back end connections.[13]

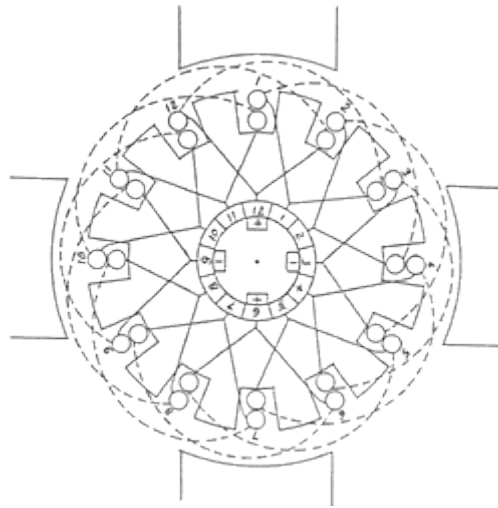


Fig 2.12 Coil sides in armature slots

2.8 Slot Pitch

Slot pitch refers to the number of slots spanned by each coil. For example, if the top of the coil in slot 1 has its bottom in slot 4, then the slot pitch is 1-4 or 3. Since the top of the coil is directly under the north pole and the bottom is directly under the south pole, the winding is known as a full pitch winding. In many cases the pitch is reduced to less than full pitch because of different reasons as per the system requirements.

2.9 Field Windings

DC machines are advantageous from a point of view of wide variety of operating characteristics which can be obtained by selection of the method of excitation of the field

windings i.e. by selection of the method of supplying current to the field windings. The field windings provide the necessary excitation required to set up the magnetic fields in the machine. The field windings may be separately excited from an external dc source or they may be self-excited i.e the machine may supply its own excitation.

(i) Separately Excited Winding

When the field is connected to an external power source, then it is known as a separately excited field.

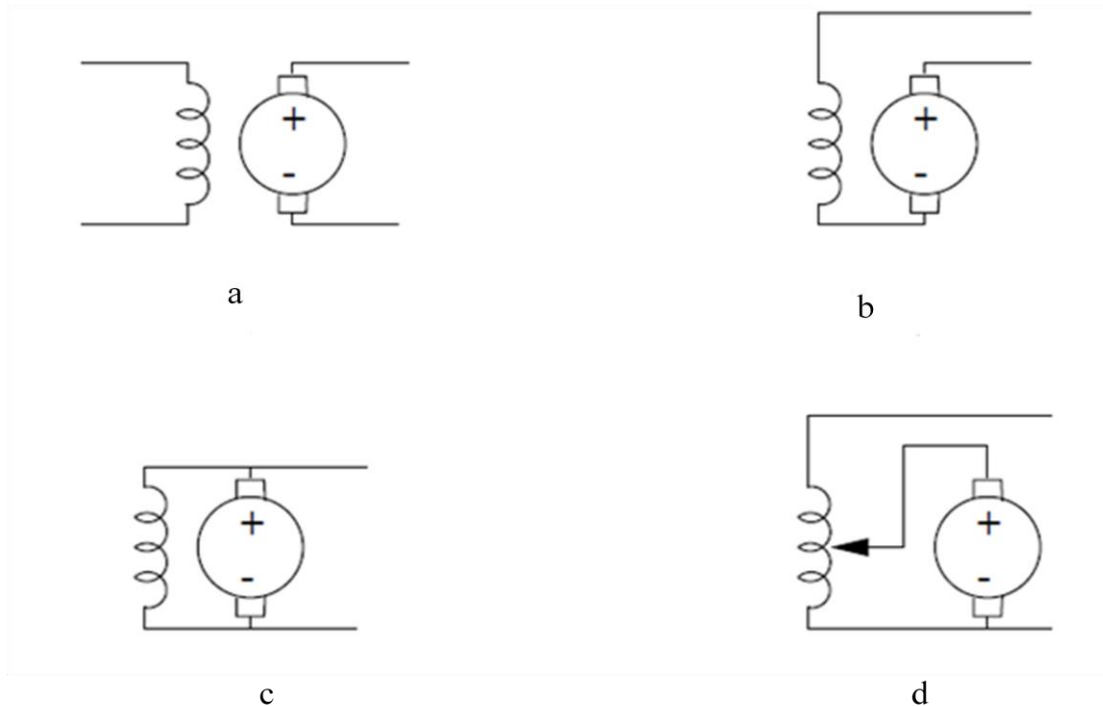


Fig 2.13 Field circuit connections of dc machines (a) separate excitation (b) series excitation (c) shunt excitation (d) compound excitation

(ii) Straight Shunt Winding

Here the winding is connected in parallel with the armature. Shunt windings consists of a large number of turns of small size wire. This winding is widely used in reversing applications as it provides the same amount of torque in both directions. The torque/ current curve is non-linear above full load. Shunt wound motors have a rising speed characteristic with increased load.

(iii) Series Winding

This winding is connected in series with the armature. A series winding consists of a small number of turns of large size wire. With this winding, the motor can produce high starting and overload torque. This design is not used for applications with light loads or no load conditions.

(iv) Compound Winding

This winding consists of a shunt winding and a series winding. This is also known as compound excitation. The series winding can be used as a starting series only or as a start and run series.

2.10 Application Areas

Industrial applications use dc motors because the speed-torque relationship can be varied as per the requirements for both dc motor and regeneration applications in either direction of rotation. Continuous operation of dc motors is commonly available over a speed range of 8:1. DC motors also possess infinite range for short durations or reduced load which proves to be very beneficial.

DC motors are applied where they momentarily deliver three or more times their rated torque. In emergency situations, dc motors can supply over five times rated torque without stalling. Dynamic braking in which dc motor-generated energy is fed to a resistor grid or regenerative braking in which dc motor-generated energy is fed back into the dc motor supply can be obtained with dc motors on applications requiring quick stops, thus eliminating the need for or reducing the size of a mechanical brake. DC motors feature a speed which can be controlled smoothly down to zero, immediately followed by acceleration in the opposite direction without power circuit switching. Another advantage of dc motors is that these respond quickly to changes in control signals due to the dc motor's high ratio of torque to inertia.

Direct current motors are unsurpassed for adjustable-speed applications and for applications where torque requirements are severe. Millions of fractional horsepower DC motors are used by the transportation industries in automobiles, trains and aircraft where they drive fans and blowers for air conditioners, heaters and defrosters; they operate windshield wipers and raise and lower seats and windows.

3.1 Introduction

All kinds of controls and control engineering is based on the foundations of feedback theory and linear system analysis and it also relates and generates the concepts of network theory and communication theory for different types of control applications. Accordingly control engineering is not limited to any engineering discipline but is applicable to aeronautical, chemical, mechanical, environmental, civil and electrical engineering. Modern control engineering practice includes the use of control design strategies and their optimal control for improving manufacturing processes, the efficiency of energy use and advanced automobile control.

A control system is an interconnection of components forming a system configuration that will provide a desired system response. The basis for analysis of a system is the foundation provided by linear system, which assumes a cause effect relationship for the components of a system as well as all non linearities within the considered system.[10]

3.2 Open Loop and Closed Loop System

An open-loop control system is controlled directly and only by an input signal. Figure 3.1 shows an open loop system. An a priori computed force is applied to the system which is expected to respond based on the specs. If the system fails to respond correctly or an unanticipated disturbance acted on it, then there is no way to correct the course. Figure 3.2 shows a feed-back system. The response $C(s)$ is measured using the sensor $H(s)$ and the resultant is compared with the input $R(s)$. The resultant difference i.e. the error is acted upon by the controller which works on the actuator. The actuator then applies the required force on the system. The closed loop thus contains the controller dynamics, the sensor dynamics, the actuator dynamics in addition to the system.

The feedback control is an operation which in the presence of disturbing forces tends to reduce the difference between the actual state of a system and an arbitrarily varied desired state of the system on the basis of this difference.

Closed loop systems can be made stable even when the open loop system is unstable by introducing artificial electronic damping into the system. Closed loop systems are relatively less sensitive to disturbances and can be made insensitive to parametric variations. [6]

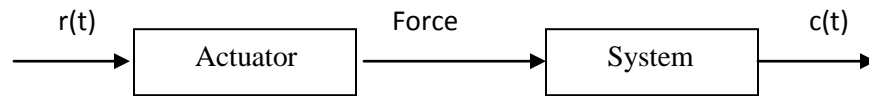


Fig 3.1 Open loop system

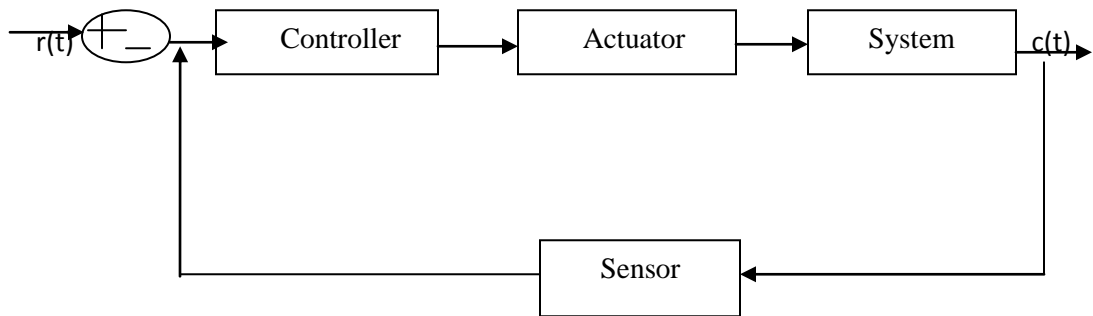


Fig 3.2 Closed loop system

The above feedback system can be shown as in figure 3.3 where the forward path controller actuator- system are shown as $G(s)$ and the return sensor path is shown as $H(s)$.

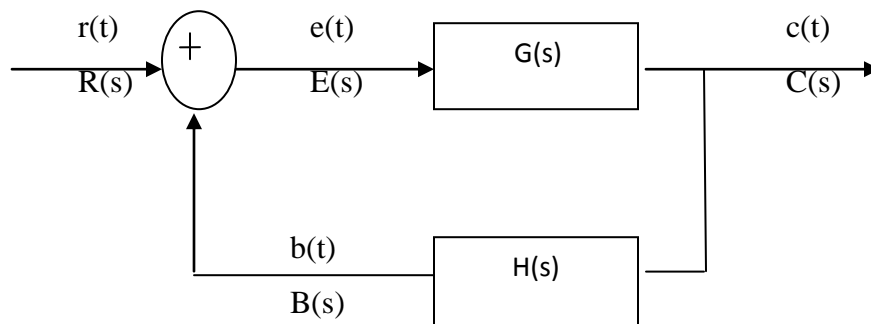


Fig 3.3 Laplace formulation of closed loop system

Where the transfer function is given as

$$\frac{C(s)}{R(s)} = \frac{G(s)}{1 + G(s)H(s)} = \frac{G(s)}{1 + G(s)} \text{ where } H(s) = 1$$

3.3 Transfer Function

A Transfer Function is the ratio of the output of a system to the input of a system. In the Laplace domain the transfer function is found while considering the initial conditions to be zero.

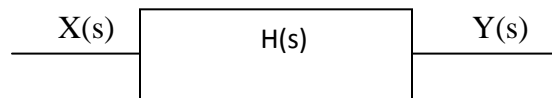


Fig 3.4 Transfer function representation

If we have an input function $X(s)$ and an output function $Y(s)$, we define the transfer function $H(s)$ to be:

$$H(s) = \frac{Y(s)}{X(s)}$$

3.4 Poles and Zeros of Open Loop and Closed Loop Systems

The closed-loop transfer function of a single-input single-output system with negative feedback is given by

$$\frac{C(s)}{R(s)} = \frac{G(s)}{1 + G(s)H(s)} = \frac{G(s)}{1 + G(s)} \text{ when } H(s) = 1$$

where $G(s)$ is the forward path

$H(s)$ is the feedback path transfer function.

The characteristic equation is obtained by setting the denominator of the closed-loop transfer function equal to zero

$$1 + G(s)H(s) = F(s) = 0$$

In order to include the multi-loop systems, let the characteristic equation of a closed loop system be expressed in its most general form i.e.

$$F(s) = 1 + L(s) = 0$$

where
$$L(s) = \frac{N(s)}{D(s)}$$

$$N(s) = K(1 + T_1s)(1 + T_2s) \dots (1 + T_ms)e^{-T_d s}$$

$$D(s) = s^p(1 + T_a s)(1 + T_b s) \dots (1 + T_r s)$$

Therefore characteristic equation can be written as

$$F(s) = 1 + L(s) = 1 + \frac{N(s)}{D(s)} = \frac{D(s) + N(s)}{D(s)} = \frac{K \prod_{i=1}^q (s + s_i)}{\prod_{j=1}^n (s + s_j)}$$

Here the poles of loop gain $L(s)$ are the poles of $F(s)$ and the zeros of $F(s)$ which are the roots of the characteristic equation of the system determine its response.

So we observe that

(i) poles of loop transfer function $L(s)$ are the poles of $F(s)$

(ii) zeroes of $1 + L(s)$ are the poles of the closed-loop transfer function and which are defined by the roots of the characteristic equation

The function $D(s)$ reveals that there are p repeated poles of $L(s)$ at $s = 0$ and r number of poles located at $s = -\frac{1}{T_a}, -\frac{1}{T_b}, -\frac{1}{T_r}$. The function $L(s)$ also has m number of finite zeros located at $s = -\frac{1}{T_i}, i = 1, 2 \dots m$ and one zero at $s = \infty$ corresponding to the delay term.

The function $F(s)$ has q number of finite zeros located at $s = -s_i, i = 1, 2 \dots q$ and n number of finite poles located at $s = -s_j, j = 1, 2 \dots n$. For a physically realizable function $F(s)$

$$n = p + r \geq q$$

3.5 Steady-State Error

Steady-state error is defined as the difference between the input and output of a system in the limit as time goes to infinity i.e. when the response has reached the steady state. The steady-state error will depend on the type of input such as step, ramp etc as well as the system whether it is type 0, type I or type II.

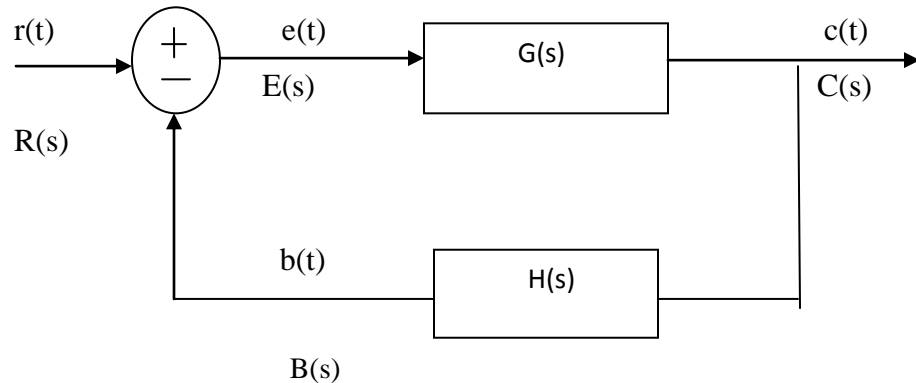


Fig 3.5 Steady state error

The steady state error for this system can be calculated from either the open or closed-loop transfer function using the final value theorem

$$T(s) = \frac{C(s)}{R(s)} = \frac{G(s)}{1 + G(s)}$$

The system output can then be expressed as

$$C(s) = R(s)T(s) = R(s) \frac{G(s)}{1 + G(s)}$$

The error $E(s)$ between the system input $R(s)$ and the system output $C(s)$ is

$$\begin{aligned} E(s) &= R(s) - C(s) \\ &= R(s) - R(s)T(s) \\ &= R(s)(1 - T(s)) \end{aligned}$$

Putting the value of $T(s)$

$$E(s) = R(s) \left(1 - \frac{G(s)}{1+G(s)} \right) = \frac{R(s)}{1+G(s)}$$

Using the final value theorem, the steady-state error is

$$e(\infty) = \lim_{s \rightarrow 0} sE(s) = \lim_{s \rightarrow 0} sR(s)(1 - T(s))$$

or

$$e(\infty) = \lim_{s \rightarrow 0} \frac{sR(s)}{1+G(s)}$$

If disturbances are considered

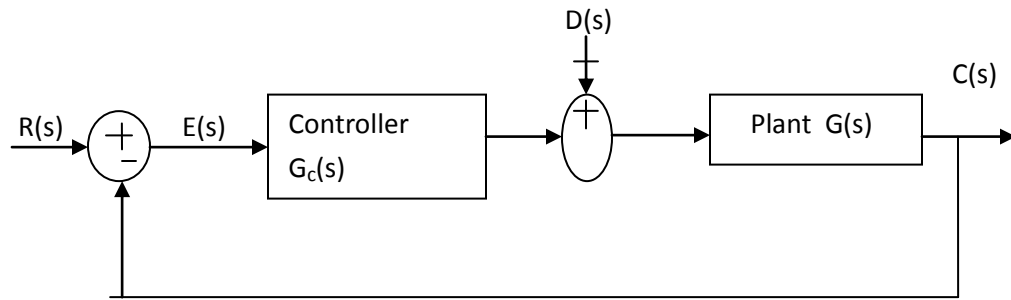


Fig 3.6 Effect of disturbances on control system

$$e(\infty) = \frac{1}{\lim_{s \rightarrow 0} \frac{1}{G(s)} + \lim_{s \rightarrow 0} G_c(s)}$$

Considering the case of step input

$$r(t) = u(t)$$

Taking Laplace

$$R(s) = \frac{1}{s}$$

Steady state error

$$e(\infty) = \lim_{s \rightarrow 0} \frac{s \left(\frac{1}{s} \right)}{1+G(s)} = \frac{1}{1+\lim_{s \rightarrow 0} G(s)}$$

3.6 State Space Representation

Modern control theory and modeling of dynamic systems is almost completely dependent upon state variable form of representation. In a state-variable representation an n th order system is described in n first-order differential equations, as opposed to a single n th order differential equation model.

State: The state of a system at any time t_0 is the minimum set of numbers $x_1(t_0), x_2(t_0), \dots, x_n(t_0)$, which along with the input to the system for $t \geq t_0$ is sufficient to determine behavior of the system for all time $t \geq t_0$. In other words, the state of a system represents the minimum amount of information that should be known about a system at t_0 such that its future behavior can be determined without reference to the input before t_0 .

x and \dot{x} are functions of time and hence are variables. These variables, which are capable of defining the state of the system, are designated as state variables.

In general an n th-order system is described by a collection of n state variables. The state variable representation is not unique, but there are infinite numbers of ways of representing state variables that can correctly describe the system dynamics.

In the state-variable formulation a continuous-data system is represented by a set of first-order differential equations called state equations.

The most general form of the system equations considered is

$$\begin{aligned}\dot{x}(t) &= Ax(t) + Bu(t) \\ y(t) &= Cx(t)\end{aligned}$$

Here x is an n -dimensional state vector, u is an r -dimensional control vector, y is an m -dimensional output vector, A is an $n \times n$ system matrix, B is an $n \times r$ control matrix and C is an $m \times n$ output matrix. In expanded form these equations become

$$\begin{bmatrix} \dot{x}_1(t) & \cdots & \vdots \\ \vdots & \ddots & \vdots \\ \dot{x}_n(t) & \cdots & \vdots \end{bmatrix} = \begin{bmatrix} a_{11} & \cdots & a_{1n} \\ \vdots & \ddots & \vdots \\ a_{n1} & \cdots & a_{nn} \end{bmatrix} \begin{bmatrix} x_1(t) & \cdots & \vdots \\ \vdots & \ddots & \vdots \\ x_n(t) & \cdots & \vdots \end{bmatrix} + \begin{bmatrix} b_{11} & \cdots & b_{1r} \\ \vdots & \ddots & \vdots \\ b_{n1} & \cdots & b_{nr} \end{bmatrix} \begin{bmatrix} u_1(t) & \cdots & \vdots \\ \vdots & \ddots & \vdots \\ u_n(t) & \cdots & \vdots \end{bmatrix} \quad (1)$$

$$\begin{bmatrix} y_1(t) & \cdots & \vdots \\ \vdots & \ddots & \vdots \\ y_m(t) & \cdots & \vdots \end{bmatrix} = \begin{bmatrix} c_{11} & \cdots & c_{1n} \\ \vdots & \ddots & \vdots \\ c_{m1} & \cdots & c_{mn} \end{bmatrix} \begin{bmatrix} x_1(t) & \cdots & \vdots \\ \vdots & \ddots & \vdots \\ x_n(t) & \cdots & \vdots \end{bmatrix} \quad (2)$$

The state variable representation in above equations allows r inputs and m outputs. Equation (1) is a set of n first-order differential equations and is usually referred to as the plant equation whereas Equation (2) represents a set of m linear algebraic equations and is referred to as the output expression.

In its most general form the output expression appears as

$$y(t) = Cx(t) + Du(t)$$

where the term $Du(t)$ indicates a direct coupling of the input to the output.

3.7 Performance Specification of Linear Systems in Time-Domain

Transient Response Specifications

Figure 3.7 illustrates a typical unit-step response of a linear analog control system. With reference to the unit-step response, performance criteria commonly used for the characterization of linear control systems in the time domain are defined as follows

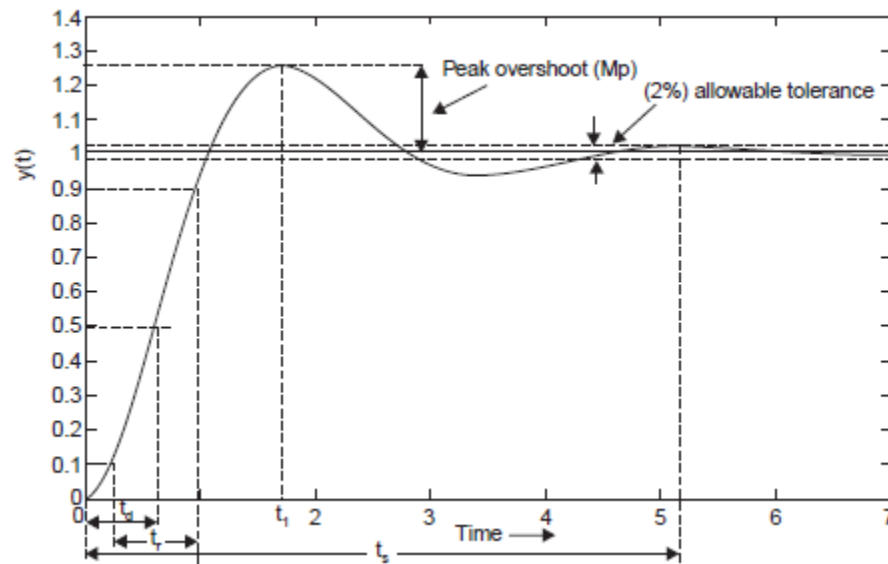


Fig 3.7 Time domain specifications

- **Maximum Percent Overshoot :**

Let y_{\max} denote the maximum value of the unit-step response $y(t)$ and y_{ss} be the steady-state value of $y(t)$ and $y_{\max} \geq y_{ss}$. The maximum percent overshoot of $y(t)$ is defined as

$$\text{Maximum percent overshoot} = \frac{y_{\max} - y_{ss}}{y_{ss}} * 100\%$$

The maximum overshoot is often used as a measure of the relative stability of the control system. A system with a large overshoot is not desirable in many applications.

- **Delay Time :**

The delay time t_d is normally defined as the time required for the step response to reach 50 percent of its final value.

- **Rise Time :**

The rise time t_r is defined as the time required for the step response to rise from 10 to 90 percent of its final value. Alternatively the rise time is defined as the reciprocal of the slope of the step response at the instant when the response is equal to 50 percent of its final value.

- **Settling Time :**

The settling time t_s is defined as the time required for the step response to decrease and stay within a specified percentage of its final value. A frequently used figure is 5 percent and 2 percent.

The above quantities give a direct measure of the transient characteristics of a control system in terms of the unit-step response

3.8 Bode Diagrams

A Bode plot is the representation of the magnitude and phase of $G(j\omega)$ where the frequency vector ω contains only positive frequencies.[22] The complex function $G(j\omega)H(j\omega)$ may be represented by two separate graphs-one giving the magnitude versus frequency and the other defining the phase angle taken in degrees versus frequency. In most of the cases the logarithm of the magnitude $G(j\omega)H(j\omega)$ is employed in bode diagram and the frequency is also plotted in logarithmic scale both for the amplitude as well as the phase angle. In general different types of plots are:

(i)Bode diagram

(ii)Polar plot

(iii)Log-magnitude versus Phase plot

The standard representation of the logarithmic magnitude of $G(j\omega)H(j\omega)$ is $20 \log |G(j\omega)H(j\omega)|$ where the base of the logarithm is 10. The unit used in this representation of the magnitude is the decibel abbreviated as dB. In the logarithmic representation, the curves are drawn on semi-log paper using the log scale for frequency and the linear scale for either magnitude or phase angle.

The advantage of using logarithmic plot for the frequency response of transfer function is that multiplication of magnitudes contributed by individual factors can be converted into addition. Furthermore it permits a simple method for obtaining an approximate log-

magnitude curve of the transfer function. It is based on straight-line asymptotic approximations which is adequate for the rough sketch of the frequency response characteristics needed in the design stage. And when exact curves are needed corrections can be easily incorporated to these basic asymptotic plots. The use of logarithmic scale makes it possible to display both the low-frequency and high-frequency characteristics of the transfer function in one graph. Even though zero frequency cannot be included in the logarithmic scale since $\log 0 = -\infty$, but we can approach easily to low frequency as is required for analysis and design of practical control system.

To plot bode plot Gain, Integral and Derivative terms $(j\omega)^{\pm 1}$, first order factors $(1 + j\omega T)^{\pm 1}$, quadratic factors $(1 + 2\delta(\frac{j\omega}{\omega_n}) + (\frac{j\omega}{\omega_n})^2)^{\pm 1}$ should be known. Using the logarithmic plots of these basic factors, it is possible to utilize them in constructing a composite logarithmic plot for any general form of $G(j\omega)H(j\omega)$ by sketching the curves for each factor and adding individual curves graphically.

The steps required to sketch the Bode plot of any transfer function are:

- Rewrite the sinusoidal transfer function as a product of basic factors.
- Plot the asymptotes for each factor on both the log magnitude and phase plots.
- Graphically add the effect of each factor.
- Make the required corrections to obtain a sketch of the exact curves.

3.8.1 Stability Analysis with Bode Plots

Bode plots are extensively used to obtain a measure of the systems stability. In order to define stability defining some basic terms:

(i)Phase Crossover: A phase crossover on the open-loop transfer function is a point where the phase plot crosses the -180° line.

(ii)Phase Crossover Frequency: The phase crossover frequency ω_p is the frequency at the phase crossover point i.e. where the phase is -180° .

(iii)Gain Margin: Gain margin is the amount of gain in dB that can be added to the open loop before the closed-loop system becomes unstable. This can easily be determined from Bode plots as the gain at the phase crossover frequency.[33]

(iv)Gain Crossover: The gain crossover is a point at which the magnitude of the gain is 0dB.

(v)Gain Crossover Frequency: The gain-crossover frequency ω_g is the frequency at the gain crossover point.

(vi)Phase Margin: Phase margin is the phase change of the open-loop transfer function required to make the closed-loop system unstable. This can easily be read off a Bode plot from the phase change at the gain crossover frequency.

Based on the above definitions the following conclusion can be drawn about the stability of closed-loop systems

- The gain margin is positive and the system is stable if the magnitude of the open-loop transfer function at phase cross over is negative in dB. That is the gain margin is measured below the 0-dB line. If the gain margin is measured above the 0 dB line, the gain margin is negative and the system is unstable.
- The phase margin is positive and the system is stable if the phase of the open-loop transfer function is greater than -180° at gain crossover. That is the phase margin is measured above the -180° line. If the phase margin is measure below the -180° line, the phase margin is negative and the system is unstable.

3.9 Root Locus

In an engineering system we typically have more than one design parameters, adjustments or user settings. It is important to determine if any of these will make the system unstable. For example think of a washing machine that vibrates so much that it ‘walks’ across a floor or a high speed aircraft that fails due to resonant vibrations. Root-locus plots are used to plot the system roots over the range of a variable to determine if the system will become unstable or oscillate.

The root-locus method has been established as a useful tool for the analysis and design of linear time-invariant control systems. The root-locus diagram is a graphical plot of the loci of the roots of the characteristic equation of a system as a function of a real parameter K which varies from $-\infty$ to $+\infty$. It gives an indication of the absolute stability and to some extent the relative stability of a control system with respect to the variation of the system parameter K.[2]

Because of the close correlation of transient responses with the roots of the characteristic equation of a system, we will study the effect of varying some design parameters on the

variation of the roots. For example when the roots lie on the negative real axis, the transient response does not exhibit any overshoot or undershoot but the response is somewhat sluggish. And if a pair of roots lies on the imaginary axis, the transient response exhibits sustained oscillations. If more than one pair of roots lie on the imaginary axis or any root has positive real part, the transient response is unbounded and the system is unstable.

3.9.1 Root-locus Drawing Rules

There is no set of rules which results in a perfect root-locus diagram. But there are certain rules which can give some information about its shape and which in turn define the system parameters.

- Firstly draw a complex plane. In this plane draw all the poles and zeroes of $G(s)H(s)$. Let us denote the n poles by a cross x and the m zeroes by a circle o .
- Determine the points on the real line which are the part of the root-locus plot. Select a point on this axis. If the total number of poles and zeroes to the right of this point is odd, then this point is part of the root-locus plot and if total number of poles and zeroes to the right of this point is not odd, then this point is not a part of the root-locus plot.
- To find breakaway points which are defined as the points where the root-locus lines breakaway from the real axis can be determined by using the relation

$$K = \frac{-(s - p_1)(s - p_2) \dots \dots (s - p_n)}{(s - z_1)(s - z_2) \dots \dots (s - z_m)}$$

Apply the condition $dK/ds = 0$ and calculate the different values of s_i . To find the breakaway points substitute the values of s into the above equation. When certain value s_i gives a positive K , then s_i is a valid breakaway point.

- To find the asymptotes, asymptote center has to be located. It is located at the point.

$$S = \frac{z_1 + z_2 + \dots + z_m - p_1 - p_2 - \dots - p_n}{n - m}$$

From this point draw asymptote lines in $n - m$ direction where $n - m$ are the number

of infinite zeroes of $G(s)H(s)$. These directions have angles

$$A = \frac{\pm(2K+1).180}{n-m}$$

When $|s|$ tends to infinity the root-locus plots will converge to these asymptotes.

- To find the points where the root-locus plot crosses the imaginary axis put $s = \omega_i$. Inserting this condition into the characteristic equation and then find a complex equation. Equating both the real and complex parts of this equation calculate ω .
- Finally we can determine the angle of departure/angle of arrival of the complex poles/zeroes which works if $G(s)H(s)$ has complex poles or zeroes. Argument equation can be used for this. Let's suppose we want to find the angle of departure/arrival of the pole p_1 . For this examine some point s_a , infinitely close to p_1 and at an angle $\arg(s_a - p_1)$. Putting this into the argument-equation, we get

$$\begin{aligned} \arg(s_a - z_1) + \dots + \arg(s_a - z_m) - \theta - \arg(s_a - p_2) \dots - \arg(s_a - p_n) \\ = (2K + 1).180 \end{aligned}$$

Since s_a is infinitely close to p_1 , simply substitute $s_a = p_1$ in the above equation and solving for the angle of departure at this pole.

So these are the some general rules which help us to draw root loci plot. For simplicity draw only one half of the graph, since root-locus plots are always symmetric about the real axis.

3.9.2 System stability

The stability of a linear system may be determined directly from its transfer function. An n th order linear system is asymptotically stable only if all of the components in the homogeneous response from a finite set of initial conditions decay to zero as time increases. If any pole has a positive real part there is a component in the output that increases without bound, causing the system to be unstable. In order for a linear system to be stable, all of its poles must have negative real parts, that is they must all lie within the left-half of the s -plane. An unstable pole, lying in the right half of the s -plane, generates a component in the system homogeneous response that increases without bound from any

finite initial conditions. A system having one or more poles lying on the imaginary axis of the s -plane has non-decaying oscillatory components in its homogeneous response and is defined to be marginally stable.

3.10 Lag Compensators

The most important thing for the design of the controller to control one process or a system is to select the controller that suits to the process. Selecting the appropriate controller that is suitable for the process is a very crucial task. The simplest method to design control is to offset the bad pole point or the zero point of the process using the controller but this method is actually impossible to execute. It is because values of the pole point and the zero point of the transfer function that are acquired from the actual process are not the very accurate and the order of the actual process may be higher. In addition the location of the pole point or the zero point is changed in accordance with the change of the variables in the actual process. Therefore it is recommendable to design the controller to move the root to the desired location instead of directly offsetting the pole point and the zero point of the process. So root locus graph is the best technique for the selection of the controller. The first phase that adjusts the system in order to get the satisfying result is to set up the gains on the root locus. But it is not sufficient to adjust only the gains when the system is changed to satisfy the defined specification. By increasing the gain the steady state movement can be improved but this may lead to unstable system. So it is required to redesign the system -- reconstruct or add devices or components in order to make the system operated as required. The device to be added for the purpose of satisfying the specification is the compensator. The compensator compensates the insufficient performance of the original system. A compensator is a control system that regulates another system by conditioning the input or output to that system. Compensators are typically employed to correct a single design flaw with the intention of affecting other aspects of the design in a minimal manner.

Lag compensators are commonly used for classical loop shaping and as weighting functions for automated controller synthesis algorithms. In classical loop shaping compensator structures are typically cascaded to modify the gain and phase characteristics of the open-loop frequency response. These alterations are used to achieve

closed-loop performance specifications for disturbance rejection, reference following, noise rejection, and gain and phase margins. Lead and lag compensators are standard tools employed in the loop-shaping process. Lag compensators can be used to adjust frequency response by adding equal numbers of poles and zeroes to systems.[26] These added singularities can be manipulated to give better stability, better performance and general improvement.

3.10.1 Approaches to System Design

The performance of a control system can be described in terms of the time domain as well as in frequency-domain parameters. The time-domain parameters include the peak time t_p , maximum overshoot and settling-time for a step input, the maximum allowable steady-state error for typical test inputs and disturbance inputs. In time-domain analysis the system behavior is associated with the location of the roots of the characteristic equation of the closed loop system. So the location of the poles and zeros of closed loop system may be specified for desired transient and steady state response. The root locus diagram may be used as a design tool when there is only one parameter normally the forward path gain is to be adjusted. But when the root cannot be placed at the desired location with a single parameter variation, lag-lead compensators are incorporated at suitable location in the structure of the system to meet the design specifications.

The performance measure of a feedback control system is also described in terms of frequency-domain parameters. The common frequency-domain parameters are the peak frequency response M_p , the resonant frequency ω_r , the bandwidth and the phase margin and gain margin of the closed loop system. A suitable compensation network can be added when the basic system fails to meet the system specifications. Bode diagram or the Nichols chart are used to design the compensator in the frequency domain. The Bode diagram are more advantageous than the Nichols chart since the contribution from the poles and zeros of the compensator becomes additive in the log scale. The Nichols chart may be used for checking the frequency response of the closed loop system at the final stage.

3.10.2 Basic Design Requirements

The nature of compensation depends upon given plant. The compensator may be an electrical, mechanical, hydraulic, pneumatic or other type of device or network. The

compensator transfer function may be placed in cascade with the plant transfer function-cascade or in series compensation and in the feedback path-feedback or parallel compensation. The next step is to select the structure of the compensator and then to obtain the parameters of compensator that satisfy the selected specifications in the best possible manner. Practically most compensators require a trial and error parameter adjustment to achieve atleast an acceptable performance.

3.10.2.1 Types of Compensation

Compensation is divided into three categories cascade, feedback and feedforward compensation

(i) Cascade Compensation

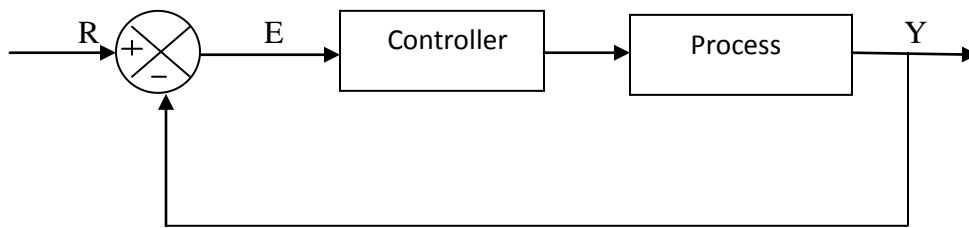


Fig 3.8 Cascade compensation

Cascade compensators are positioned to act on the error signal in a closed-loop control system to achieve the desired system performance, the most popular types of compensator being the phase-lead / phase-lag compensators.

(ii) Feedback Compensation

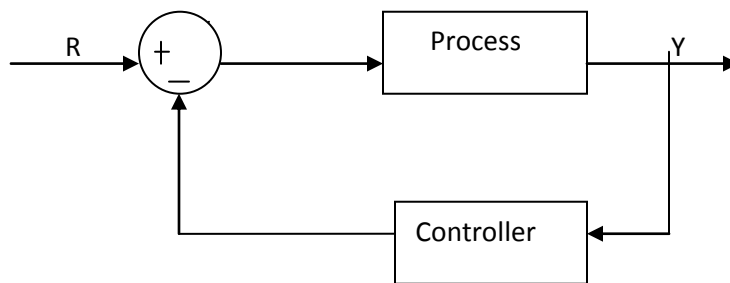


Fig 3.9 Feedback compensation

In this configuration the compensator is positioned in a feedback path the velocity and acceleration types are most common. Thus the compensator acts on the output signal to meet the desired system performance.

(iii) Feedforward Compensation

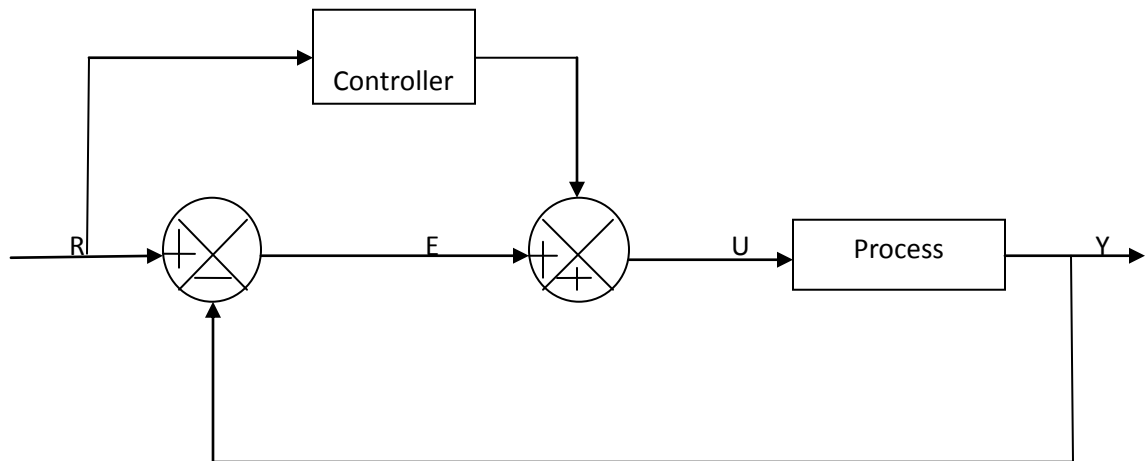


Fig 3.10 Feedforward compensation

In any control system a disturbance or load change causes an error between the controlled output and the command input. So the controller's function is to reduce/eliminate this error. But the effect of the disturbance must show up in the error before the controller can counteract it. In feedforward compensation, the disturbance is measured and a signal is added to the controller output to enhance the control law. Thus a corrective action is initiated without waiting for the effect of the disturbance to show up in the error.

3.10.3 General Rules for Lag Compensator

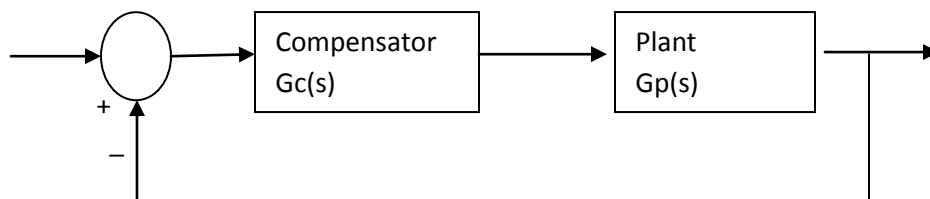


Fig 3.11 Lag compensator design

$$D(s) = K \frac{(s+z)}{(s+p)}$$

where $z > p$, for a lag compensator

- Select the control gain K to satisfy the specifications for the closed-loop poles s_1, s_2 using root-locus.
- Find the desired value for gain $K_d = D(0) = Kz/p$, using the specifications for e_{ss} .
- Find the lag ratio $\alpha = z/p = k_d/k > 1$.
- Select the lag compensator's zero z , 4 to 10 times to the right of the dominant closed-loop poles.
- Find the lag compensator's pole $p = z/\alpha$.
- Check the closed-loop system's specifications.

3.11 PID Control

“PID” is an acronym for “proportional, integral, and derivative.” A typical structure of a PID control system is shown in figure 3.12 where it can be seen that in a PID controller, the error signal $e(t)$ is used to generate the proportional, integral and derivative actions with the resulting signals weighted and summed to form the control signal $u(t)$ applied to the plant model. [12]

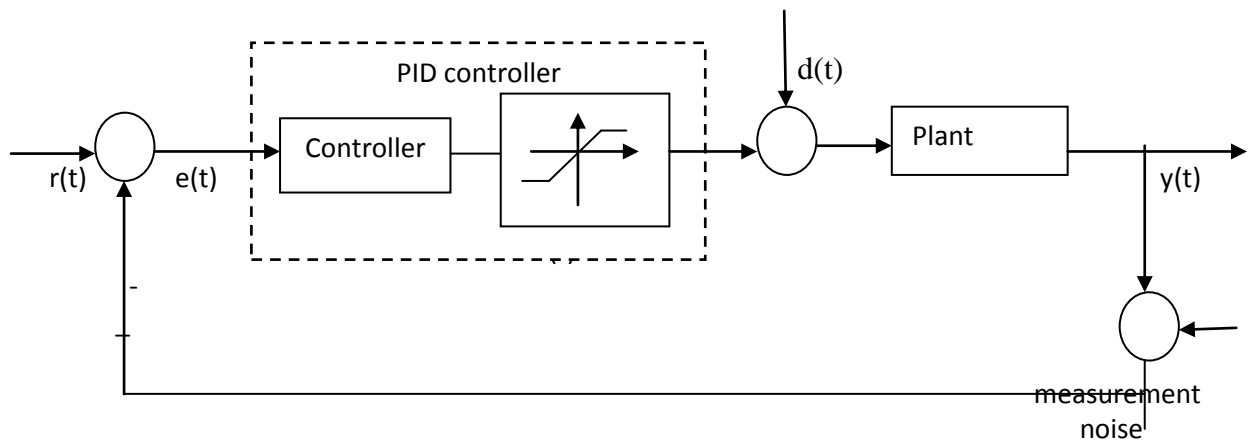


Fig 3.12 PID controller

(i)Proportional Term

The proportional term P gives a system control input proportional with the error. Using only P control gives a stationary error in all cases except when the system control input is zero and the system process value equals the desired value. In figure the stationary error in the system process value appears after a change in the desired value. Using a too large P term gives an unstable system.

(ii)Integral Term

The integral term I gives an addition from the sum of the previous errors to the system control input. The summing of the error will continue until the system process value equals the desired value and therefore there is no error when the reference is stable. The most common use of the I term is normally together with the P term called a PI controller. Using only the I term gives slow response and oscillating system. Figure shows the step responses to a I and PI controller. From figure the PI controller response have no stationary error and the I controller response is very slow.

(iii)Derivative Term

The derivative term (D) gives an addition from the rate of change in the error to the system control input. A rapid change in the error will give an addition to the system control input. This improves the response to a sudden change in the system state or reference value. The D term is typically used with the P or PI as a PD or PID controller. A too large D term usually gives an unstable system. Figure 3.13 shows D and PD controller responses. The response of the PD controller gives a faster rising system process value than the P controller. The D controller behaves as a high pass filter on the error signal and thus easily introduces instability in a system and make it more sensitive to noise.

Transfer Function of PID controller

$$u_c(t) = K_c e(t) + \frac{K_c}{T_I} \int_0^t e(\tau) d\tau + K_c T_D \frac{de(t)}{dt}$$

The controller variables are

| | |
|-------------------------|------------------------|
| $k_c = k_p$ | Gain |
| $T_I = \frac{K_p}{K_I}$ | integral action time |
| $T_D = \frac{K_D}{K_P}$ | derivative action time |

As special cases of PID controllers one obtains for:

(i) $T_D = 0$ the PI controller with transfer function

$$G_c(s) = K_c \left(1 + \frac{1}{T_I s}\right)$$

(ii) $T_I \rightarrow \infty$ the ideal PD controller with the transfer function

$$G_c(s) = K_c(1 + T_D s)$$

(iii) $T_D = 0$ and $T_I \rightarrow \infty$ the P controller with the transfer function

$$G_c(s) = K_c$$

(iv) A pure I controller may also be applied and this has the transfer function

$$G_c(s) = k_I \frac{1}{s} = \frac{K_c}{T_I s}$$

The step responses of these types of controllers are compiled in following figure

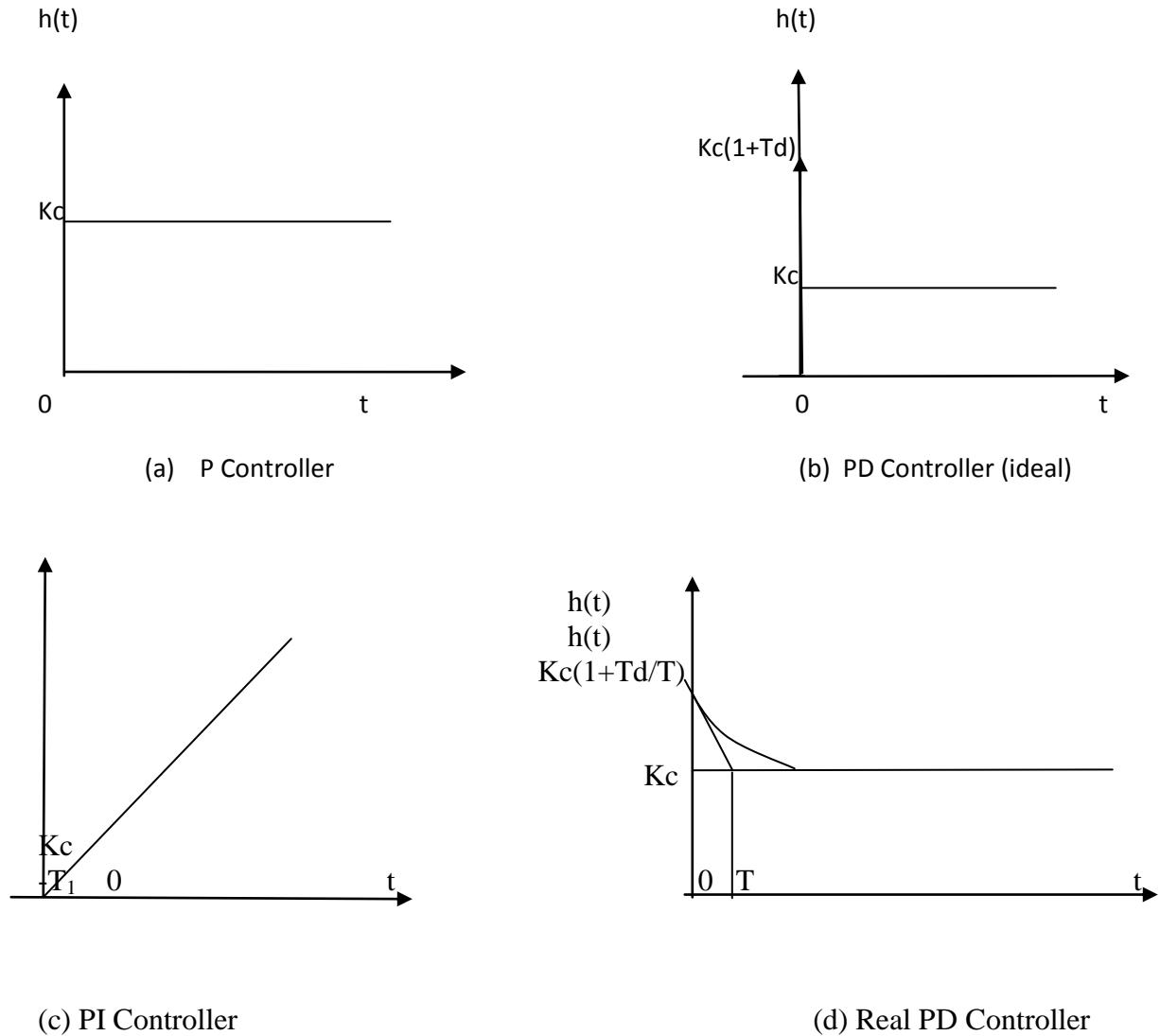


Fig 3.13 Step responses of different controllers

3.11.1 Comparison between different types of controllers

- The P controller shows a relatively high maximum overshoot a long settling time as well as a steady-state error.
- The I controller has a higher maximum overshoot than the P controller due to the slowly starting I behavior, but no steady-state error.
- The PI controller fuses the properties of the P and I controllers. It shows a maximum overshoot and settling time similar to the P controller but no steady-state error.

- The PID controller fuses the properties of a PI and PD controller. It shows a smaller maximum overshoot than the PD controller and has no steady state error due to the *I* action.

4.1 Problem Definition

DC motors are widely used in high frequency or low frequency applications. So the response of dc motors should be well defined and should be very precise. While studying the closed loop response and other parameters of dc motor it is seen that response curves are not smooth. Some disturbances are seen in the curves which are not desirable. Therefore it becomes necessary to control these parameters by some technique. The major aim while controlling the DC motor is to control the various parameters like location of poles and zeros, natural frequency, damping ratio, settling time, overshoot, peak overshoot, gain, rise time etc. The problem starts with some initial parameters of dc motor and then the parameters are modified accordingly, to obtain the desired response. The response of dc motor can be manipulated in terms of bode plots, root loci, closed loop and open loop responses. The adjustment of various parameters is very crucial because even a difference of 0.01 in gain margin or phase margin can cause the response curve to deviate from a large value which ultimately leads to poor response of dc motor. The response of dc motor is dependent upon various control system terminology for example delay time which is defined as the time required for the step response to reach 50 percent of its final value or rise time t_r which is defined as the time required for the step response to rise from 10 to 90 percent of its final value or the settling time t_s which is the time required for the step response to decrease and stay within a specified percentage of its final value. Firstly the response curves are studied in a normal case and then to get desired results or to achieve better results compensator is designed. The gain, settling time, delay time, overshoot, peak overshoot of compensator are chosen by hit and trial method keeping track of desired response. Bode plots and root loci are the best tools to study such responses. Root loci are specifically used to locate the position of zeros and poles and thus shifting of root loci curve is analyzed. On the other hand Bode Plots in which the complex function $G(j\omega)H(j\omega)$ can be represented by two separate graphs, one giving the magnitude versus frequency and the other the phase angle versus frequency proves to be a good tool for analyzing the behavior of DC motor. Furthermore Bode plots

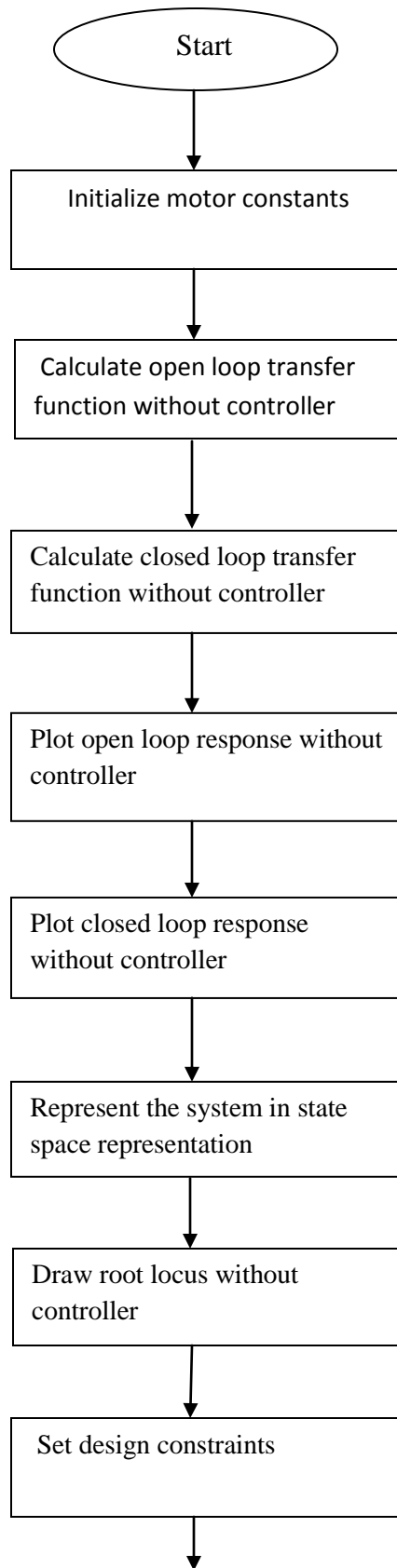
permits a simple method for obtaining an approximate log-magnitude curve of the transfer function. It is based on straight-line asymptotic approximations, which is adequate for the rough sketch of the frequency response characteristics needed in the design stage. And when exact curves are needed, corrections can be easily incorporated to these basic asymptotic plots. Further the filters like notch filter can also be added with suitable specifications along with compensator in order to filter the little disturbances that may exist in the output stage after implementation of compensator.

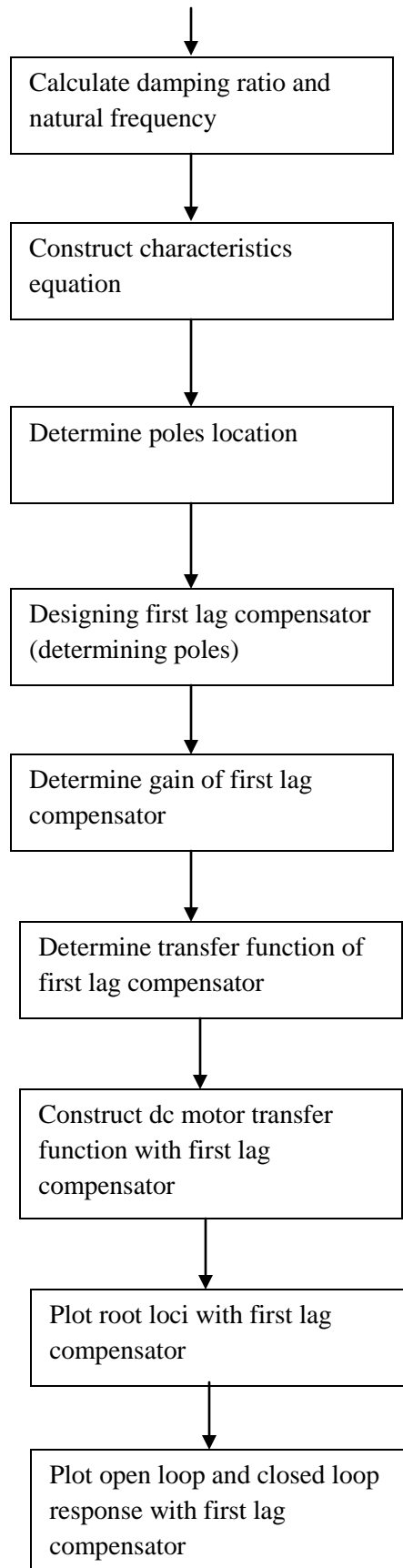
Compensator plays a major role in improving the response of dc motor. So choosing the suitable parameters for compensator in order to get desired response is a very crucial stage. Various types of compensator can be designed for example lag compensator, lead compensator. In this thesis work lag compensator is designed with suitable parameters.

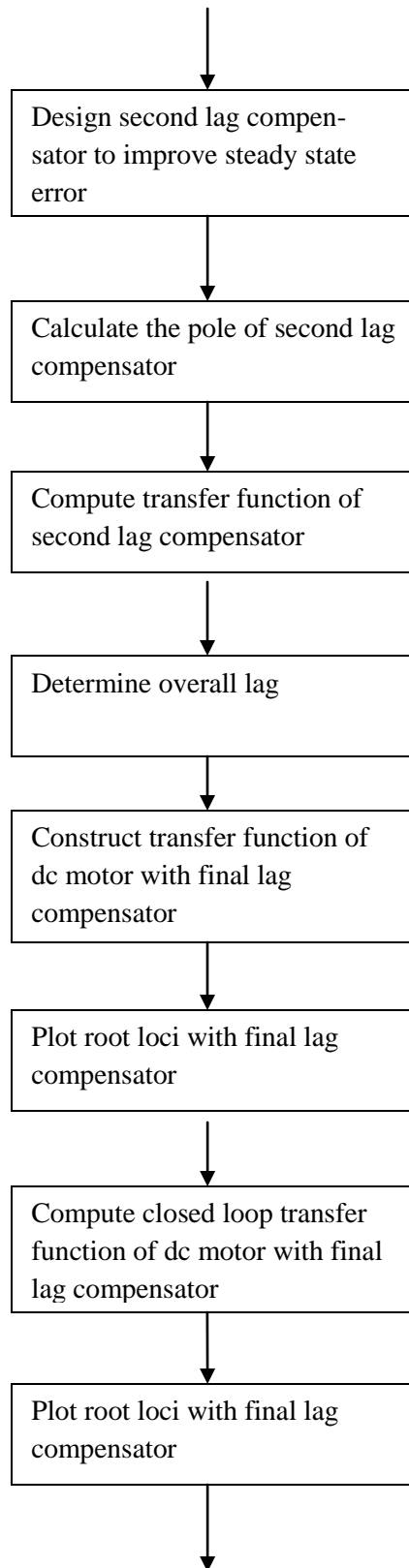
Matlab is being used in order to design the compensator. The poles, zeroes, transfer function of desired lag compensator are calculated and the corresponding open loop response, closed loop response, root loci are plotted by taking some initial values of DC motor constants. The results are analyzed in terms of time constants, peak overshoot etc. The stability of the system is determined by the location of the roots in root loci plot. Then another lag compensator is designed and on the similar basis roots are plotted on root loci plot and thus response is analyzed continuously and this process goes on until we get precise results.

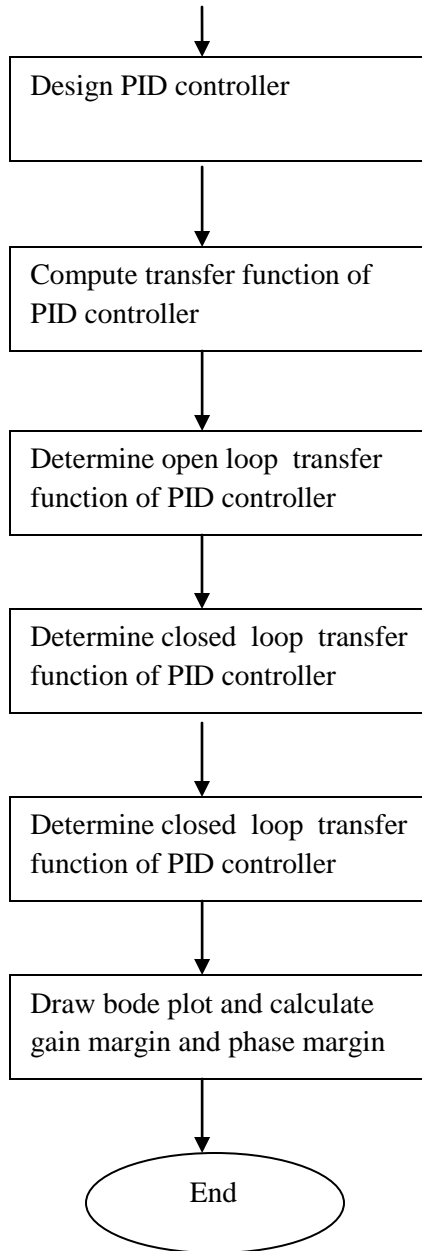
4.2 Implementation

To design lag compensator the Matlab is being used. Matlab-Matrix Algebra laboratory, distributed by The MathWorks, is a technical computing environment for high performance numeric computation and visualization. It integrates numerical analysis, matrix computation, signal processing, and graphics in an easy-to-use environment. Matlab also features a family of application-specific solutions called toolboxes. Toolboxes are comprehensive collections of Matlab functions that extend its environment in order to solve particular classes of problems. The complete steps required to evaluate the problem are shown in following flowchart:









CHAPTER 5

RESULTS AND DISCUSSIONS

The complete algorithm of the design proposed is being presented in this chapter and the corresponding results have been discussed.

(i) Firstly the motor constants like damping ratio, resistance, inductance, damping constant are initialized. The values chosen are $J=0.02$, $b=0.2$, $k_t=0.02$, $k_e=0.02$, $R=2$, $L=0.4$ and to design PID controller assumed values are $K_p=70$, $K_i=170$, $K_d=5$.

(ii) Using Matlab compute the open loop transfer function without controller by defining numerator and denominator using the above defined values. The transfer function is obtained as

$$H(s)_{\text{open loop}} = \frac{0.02}{0.008s^2 + 0.12s + 0.4004}$$

(iii) By introducing feedback in the Matlab command compute the closed loop transfer function.

$$H(s)_{\text{closed loop}} = \frac{0.02}{0.008s^2 + 0.12s + 0.4204}$$

(iv) Plot the open loop response without controller by choosing suitable scale on the axes. Keep grid on so that it becomes easier to analyze the curve.

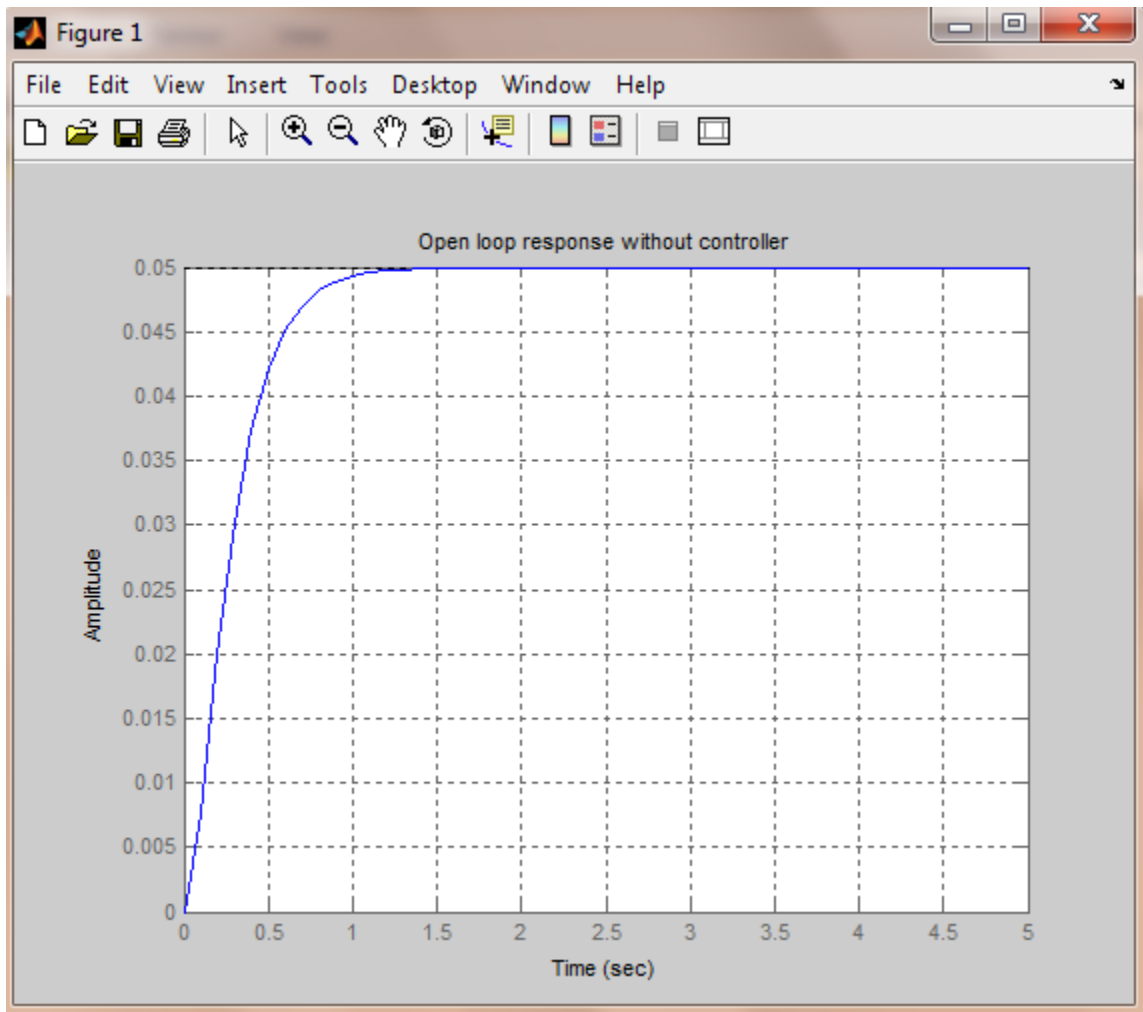


Fig 5.1 Open loop response without controller

(v) On similar basis plot the closed loop response without controller.

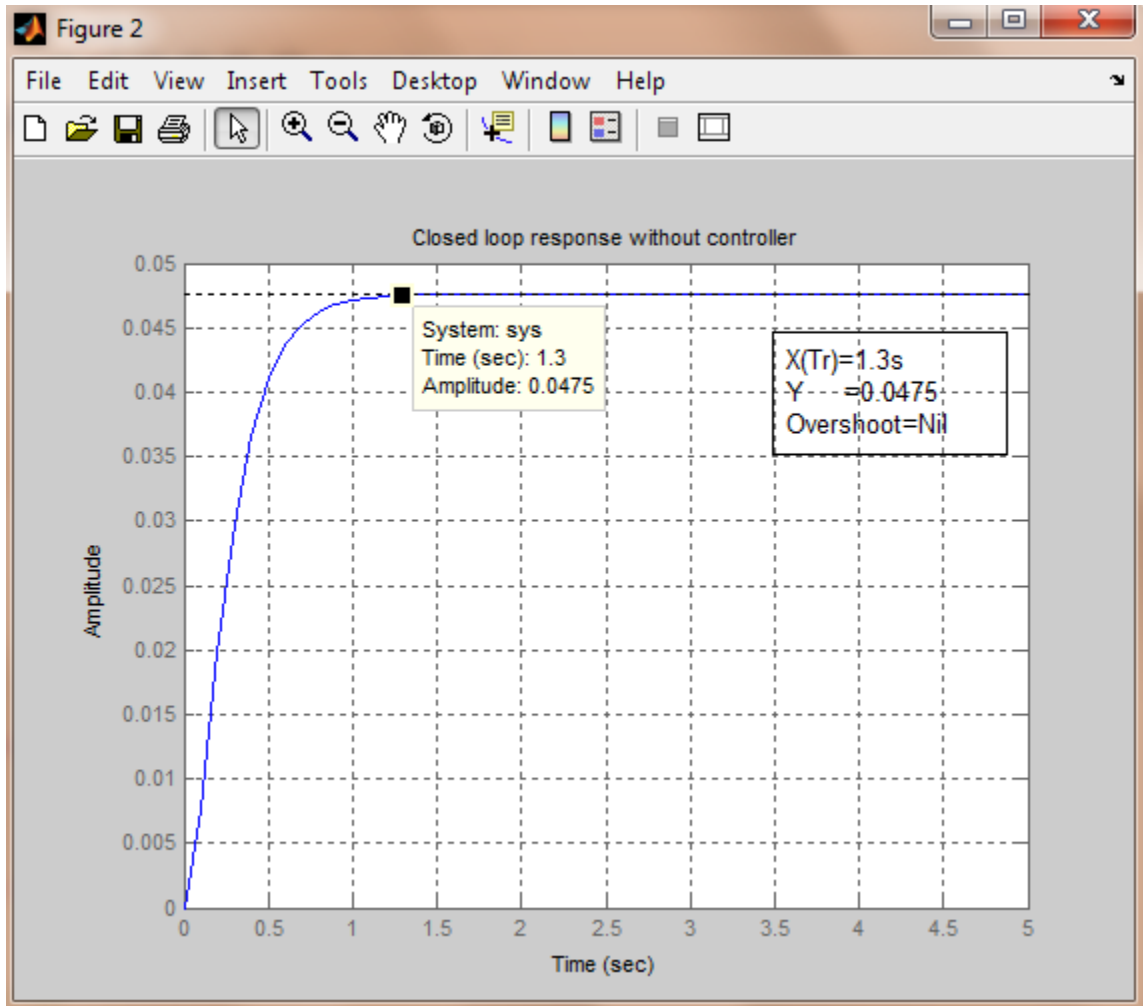


Fig 5.2 Closed loop response without controller

(vi) Represent the system in state space representation in terms of state variables and state matrices.

```
Command Window
i New to MATLAB? Watch this Video, see Demos, or read Getting Started.

State Space representation:

a =
      x1      x2
x1   -5  -0.05
x2    1   -10

b =
      u1
x1   2.5
x2    0

c =
      x1  x2
y1    0   1

d =
      u1
y1    0

Continuous-time model.
```

Fig5.3 : State space representation

(vii) Plot root locus without controller using above computed transfer function as and keeping grid on. The plot obtained is shown below:

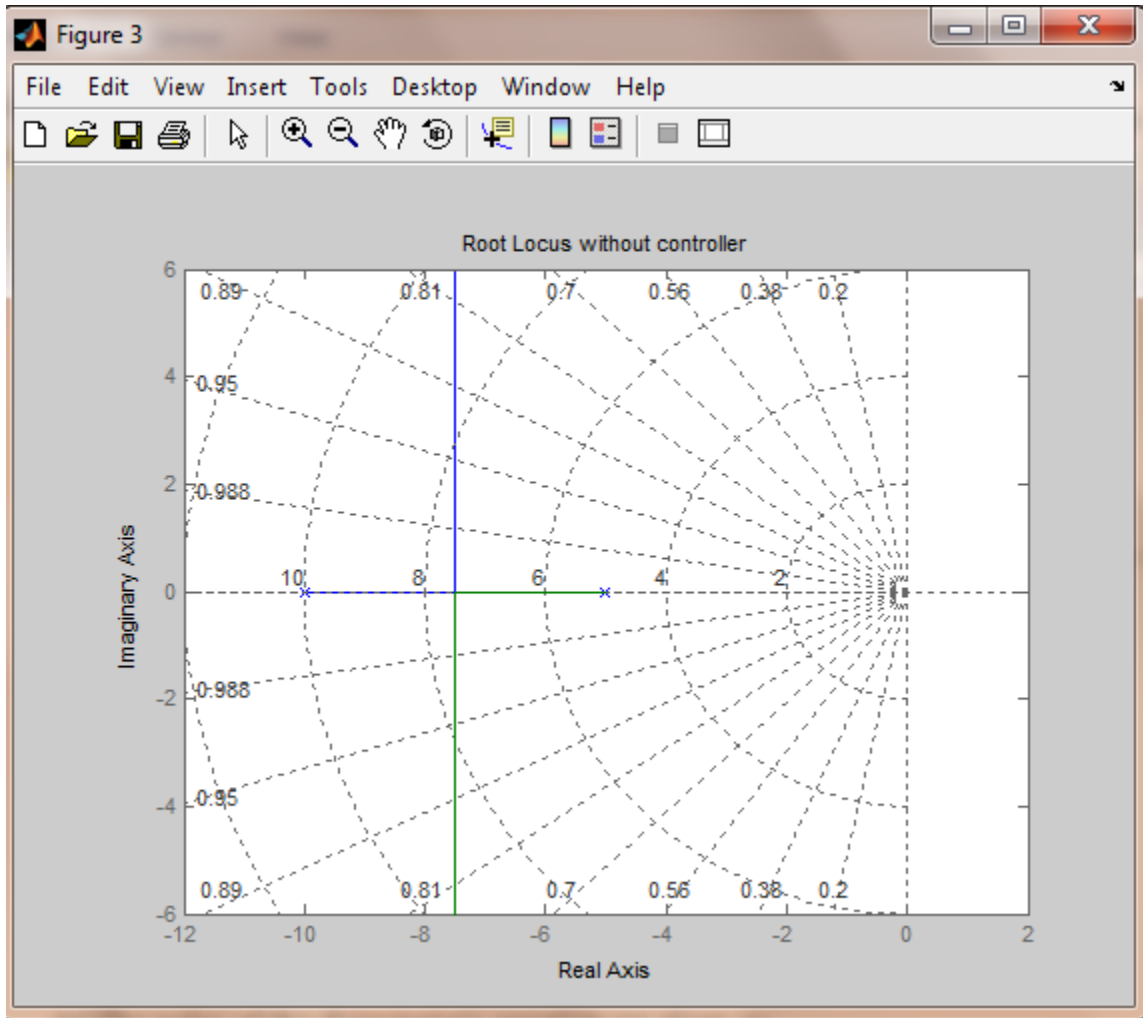


Fig 5.4 Root locus without controller

(viii) Set design constraints as settling time less than 1%, overshoot < 5%, steady state error < 0.4%

(ix) The damping ratio and natural frequency of the system comes out to be

$$\text{Damping Ratio} = 0.6901$$

$$\text{Natural Frequency} = 5.7962$$

(x) The characteristic equation of the system is given as

$$1.0 \quad 8.0000 \quad 33.5960$$

(xi) The poles of the characteristic equation are given as:

$$-4.0000 + 4.1948i \quad -4.0000 - 4.1948i$$

(xii) To design lag compensator assume zero of lag compensator as 14.

(xiii) The pole and gain of first lag compensator

$$\text{Pole of first Lag Compensator} = 3.9054$$

$$\text{Gain of first Lag Compensator} = 4.8832$$

(xiv) The transfer function of first lag compensator in order to improve settling time and overshoot is computed as

$$H(s) = \frac{4.883s + 68.36}{s + 3.905}$$

(xv) DC motor transfer function with lag compensator

$$H(s) = \frac{12.21s + 770.9}{s^3 + 18.91s^2 + 108.6s + 195.5}$$

(xvi)The root loci plot with first lag compensator is obtained as

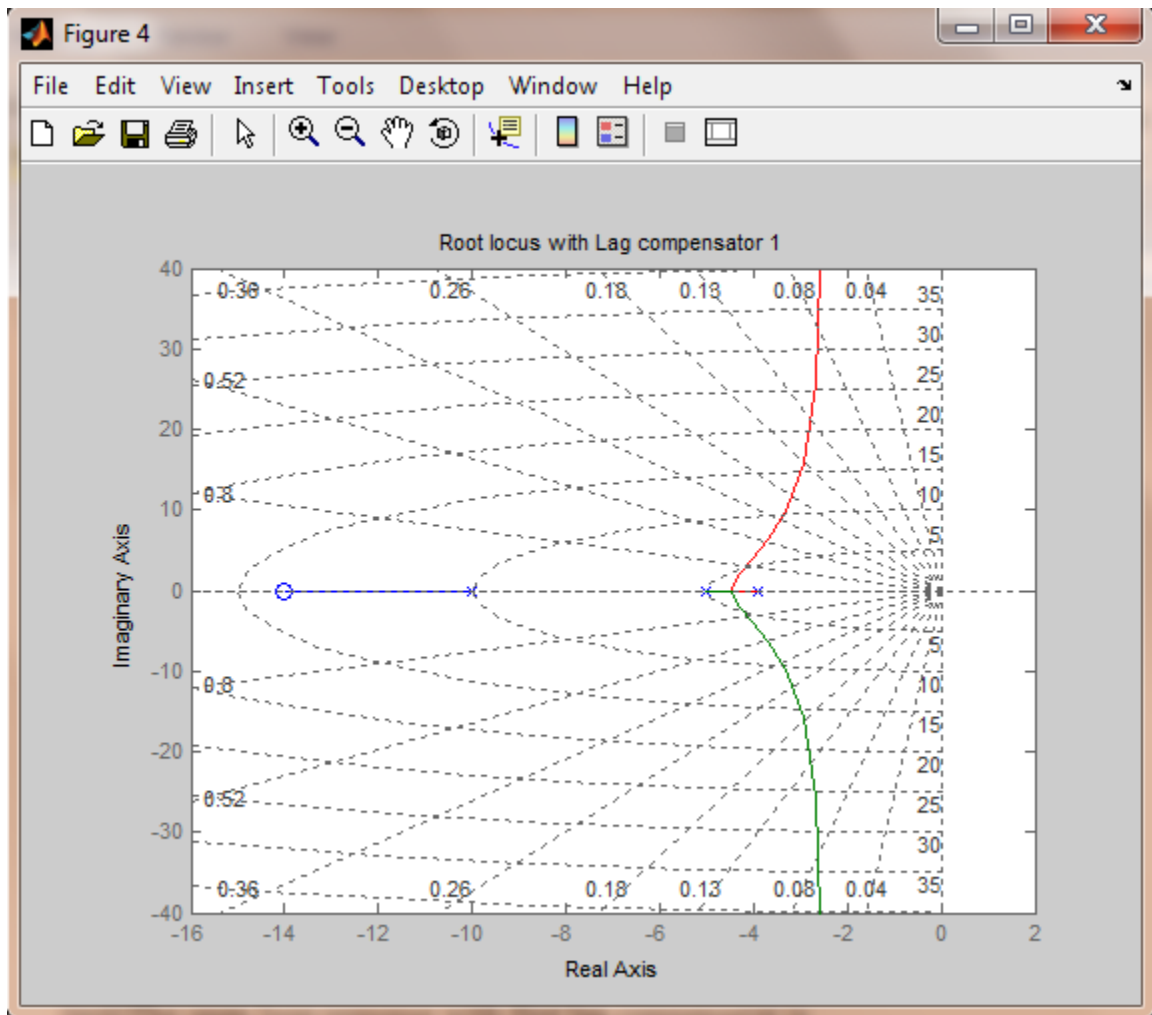


Fig 5.5 Root locus with first lag compensator

(xvii)The open loop response with first lag compensator is

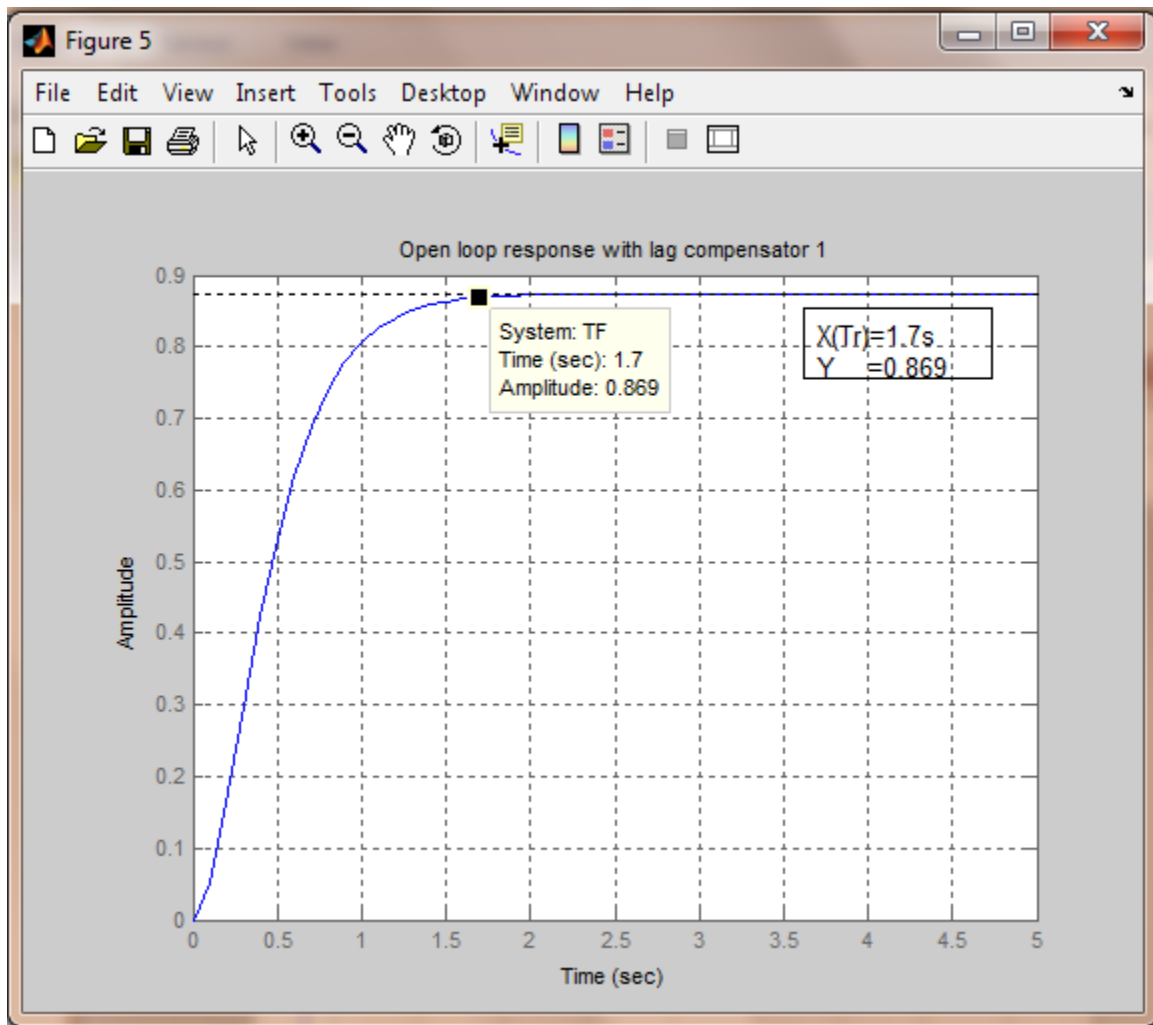


Fig 5.6 Open loop response with first lag compensator

(xviii)The closed loop response plot with lag compensator comes out to be

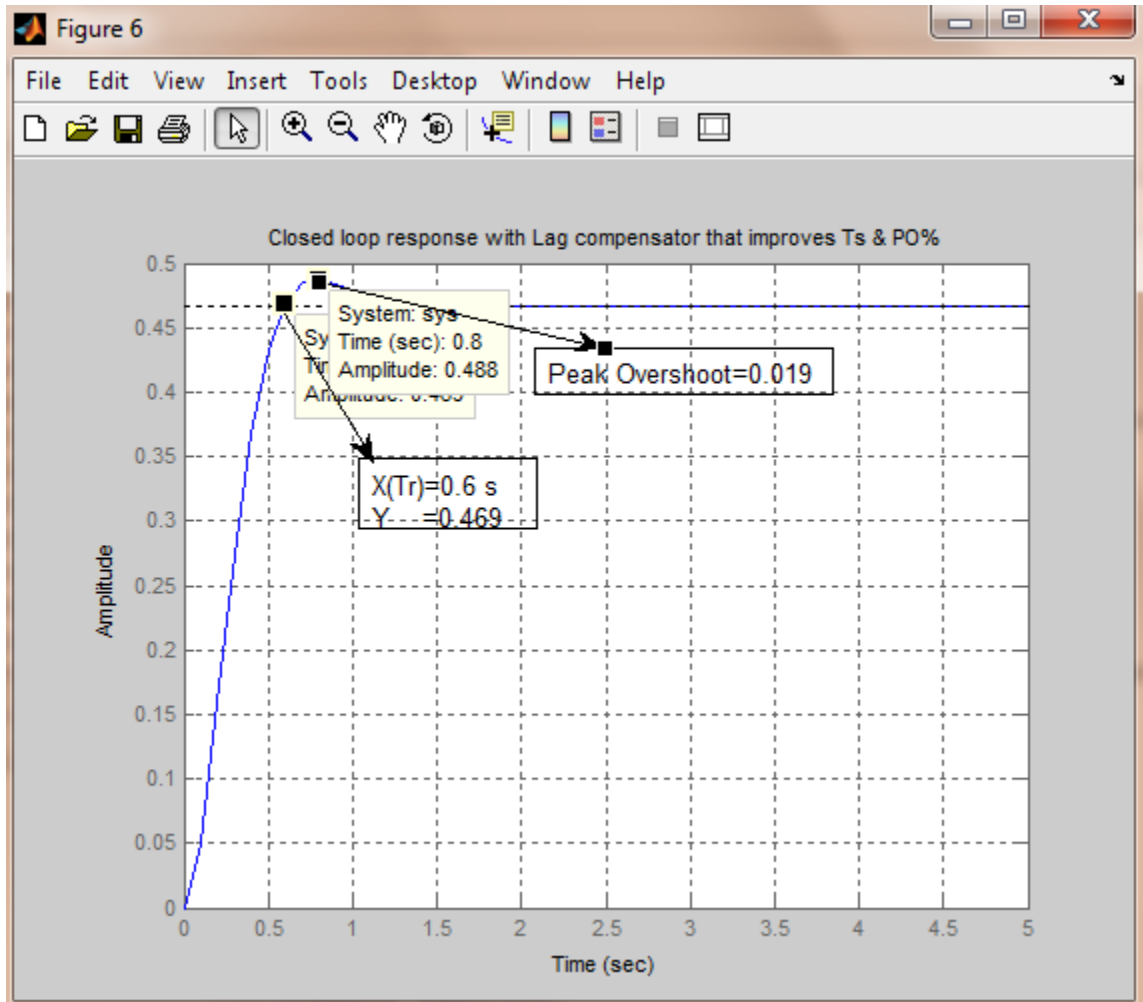


Fig 5.7 Closed loop response with first lag compensator

(xix)To improve further steady state error second lag compensator is being designed. Assuming zero of second lag compensator as 2.9 and steady state error as 0.004, the pole of second lag compensator comes out to be 0.0217.

(xx)The transfer function of second lag compensator in order to improve steady state error is computed as

$$H(s) = \frac{s+2.9}{s+0.02174}$$

(xxi)The overall lag compensator transfer function (lag1*lag2) is

$$H(s)_{\text{overall}} = \frac{4.883s^2+82.53s+198.3}{s^2+3.927s+0.08491}$$

(xxii)Open loop transfer function of dc motor with final lag compensator is

$$H(s)_{\text{ol(dc)}} = \frac{12.21s^2+206.3s+495.6}{s^4+18.93s^3+109s^2+197.8s+4.25}$$

(xxiii)The root locus plot with final lag compensator is obtained as

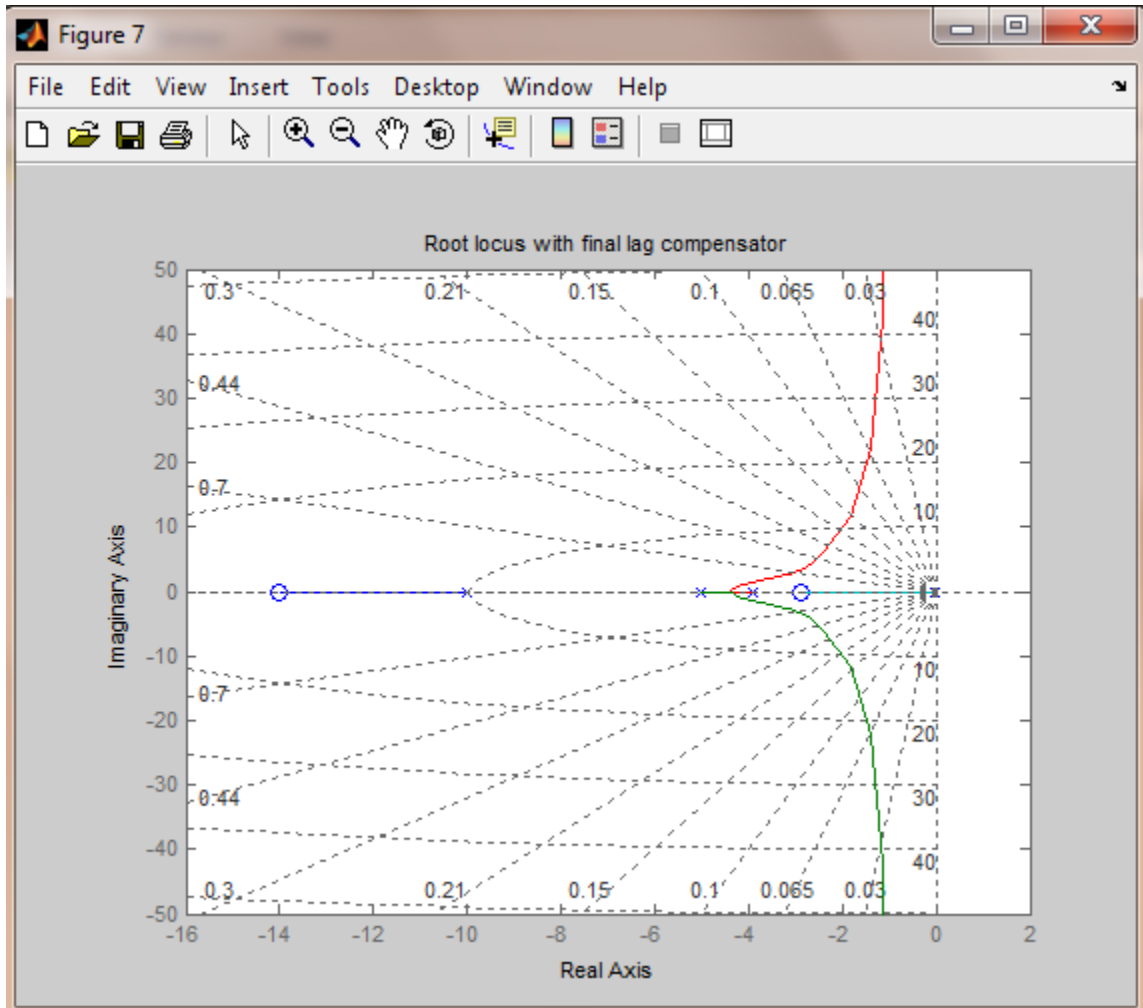


Fig 5.8 Root locus with final lag compensator

(xxiv)The closed loop transfer function of DC motor with final lag compensator

$$H(s)_{cl(dc)} = \frac{12.21s^2 + 206.3s + 495.6}{s^4 + 18.93s^3 + 121.3s^2 + 404.1s + 499.9}$$

(xxv) The closed loop response of dc motor with PID controller is shown as below

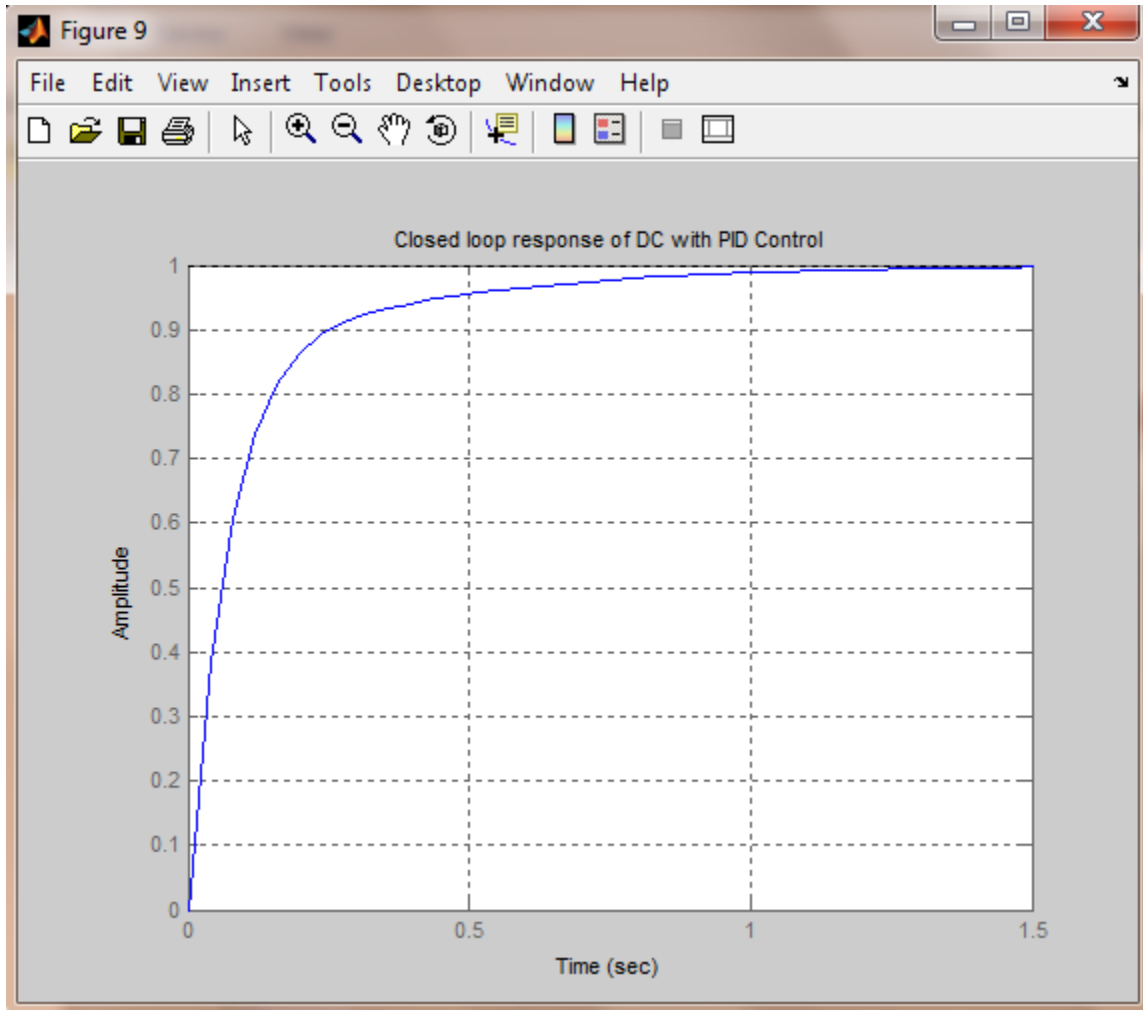


Fig 5.9 Closed loop response of DC motor with PID control

(xxvi) To determine gain margin and phase margin bode plot is drawn and the corresponding computed values are shown in the figure

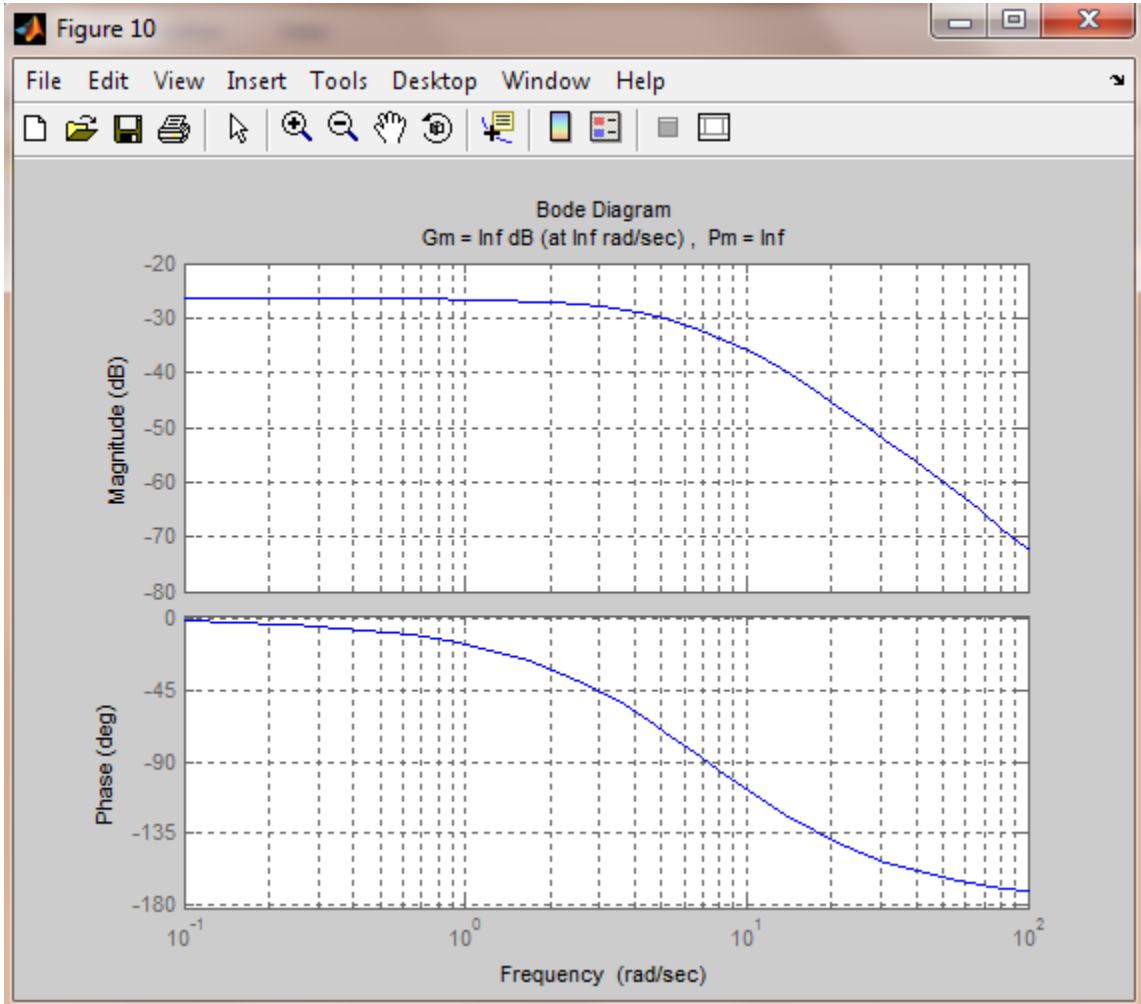


Fig 5.10 Bode plots

(xxvii) Bode plot of closed loop transfer function with lag compensator is

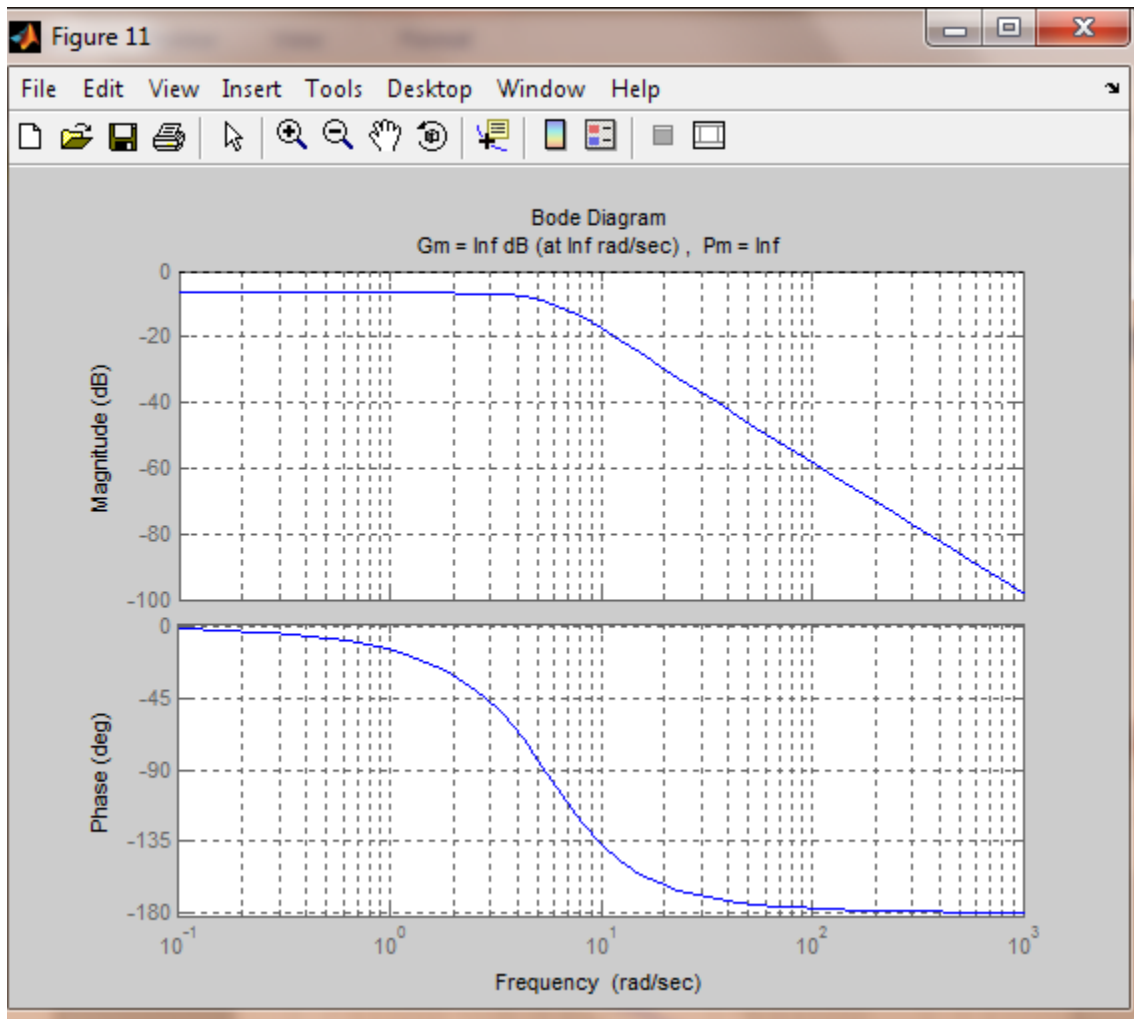


Fig 5.11 Bode plot of closed loop transfer function with final lag compensator

Conclusions

In this thesis work lag compensator is designed in order to achieve the desired results. It has been concluded that lag compensator improves the steady state behavior of the dc motor system. In addition to steady state behavior, other parameters like rise time, settling time, overshoot also get improved. By assuming the suitable values of poles and zeroes the corresponding transfer functions are constructed. The open loop and closed loop responses are also plotted and the behavior can be easily analyzed in terms of rise time, overshoot as described in the corresponding curves. To achieve the better results, lag compensator is employed and it can further be concluded that the time domain parameters get improved to a large extent. Infact the overshoot can be seen in the graph but improvement in rise time and settling time compensates for the effect of overshoot.

The stability of dc motor system can further be analyzed in terms of root loci plot. In order for a linear system to be stable all of its poles must have negative real parts that is they must all lie within left half of s-plane. It can be analyzed from the root loci plot obtained that all poles lie on left half of s-plane. As we step over from root loci plot from first lag compensator to second lag compensator, from the location of poles and zeroes it can be analyzed that the stability improves to a large extent. Bode plot are constructed in order to calculate gain margin and phase margin. Lag compensator adds negative phase to the system over the specified frequency. The values obtained of the gain and phase margins in the curves indicates that the system is inherently stable.

Thus on the overall, the designed compensator proves to be a efficient compensator for the dc motor system and with this the response of dc motor system improves significantly.

Future scope

The lag compensator with improved parameters as designed above if incorporated with a lead compensator i.e. a combination of lag-lead compensator, would result in a better system. Thus the system performance parameters will improve significantly and thus a stable system so designed can be used in a wide variety of applications.

REFERENCES

1. Marro G, Zanasi R, “New Formulae and Graphics for Compensator Design”, IEEE Transactions, pp 129- 133, 1998
2. Coelho Carlos Alberto D, “Root-Locus-based Computational Algorithms for Control System Parameter Setting”, Proceedings of the American Control Conference, pp 2037-2039, 1998
3. Hurl R Hwa, Lee Jang M, Lee Suk, Lee H Man, “Compensation of Time Delay Using a Predictive Controller”, IEEE Transactions, pp1087-1092, 1999
4. Shen J X, Tseng K J, “Analyses and compensation of rotor position detection error in a sensorless permanent magnet brushless dc motor”, IEEE Transactions, pp 81-83, 1999
5. Yeung Kai Shing, Lee Kuo Hsun, “A universal design chart for linear time invariant continuous time and discrete-time compensators”, IEEE Transactions, Vol.43, No 3, pp 309-315, 2000
6. Goodwin G C, Graebe S F, Salgado M E, “Control System Design”, New Jersey: Prentice-Hall, 2001
7. Cavicchi J Thomas, “Minimum return difference as a compensator design tool”, IEEE Transactions, Vol. 44, No 2, pp120-128, 2001
8. Kelly Rafael, Moreno Javier, “Learning PID structures in an introductory course of automatic control”, IEEE Transactions , Vol. 44, No. 4, pp 373-376, 2001

9. Wang Fei-Yue, Huang Yue, "A Non-Trial-and-Error Method for Phase-Lead and Phase Lag Compensator Design", IEEE Transactions, pp 1654-1660, 2001
10. Katsuhiko Ogata, Modern Control Engineering, 4th edition, Prentice-Hall of India 2002
11. Xu J X, Hui K E, Yang R H, " Maximum phase added lead, minimum phase reduced lag non-trial-and-error compensator design", Proceedings of 4th Asia Control Conference Singapore, pp 93-98, 2002
12. Shigemasa Takashi, Yukitomo Masanori, "A model-driven pid control system and its case studies", IEEE Transactions, pp 571-576, 2002
13. Zhu Z.Q, Ede J. D, Howe D, "Design criteria for high speed brushless dc motors for sensorless operation", International Journal of Applied Electromagnetics & Mechanics, Vol. 15, pp79-87, 2002
14. Wang F Y, "The exact and unique solution for phase lead and lag compensation", IEEE Transactions , pp 258-262, 2003
15. Godhwani Arjun, "Feedback Control Systems", IEEE Transactions, pp 1758-1761, 2003
16. Cavicchi J Thomas, "Phase Margin Revisited: Phase-Root Locus, Bode Plots and Phase Shifters", IEEE Transactions, Vol. 46, No 1, pp 168-176, 2003
17. Bianchi N, Bolognani S, Luise F, "Analysis and design of a brushless motor for high speed operation", IEEE Transactions , pp 44-51, 2003

18. C Marcelo, Teixeira M, Assuncao Edvaldo, Machado Erica R. M. D., "A method for plotting the complementary root locus using the root-locus rules", IEEE Transactions, Vol. 47, No 3, pp 405-409, 2004
19. Yang Ciann-Dong, Wei Chia-Hung, "Root-Locus Dynamics", American Control Conference, pp 63-68, 2005
20. Song Yang, Baoku Su, "A new repetitive adaptive compensation scheme in the dc motor system", IMACS Multi-Conference on "Computational Engineering in Systems Applications", pp1140-1143, 2006
21. Cmosija Petar, Krishnant Ramu, Toni Bjazic, "Optimization of PM brushless dc motor drive speed controller using modification of ziegler- nichols methods based on bode plots", IEEE Transactions, pp 343-348, 2006
22. Emami Tooran, Watkins John M, Richard T. O'Brien, "A unified procedure for continuous-time and discrete-time root-locus and bode design", IEEE Transactions, pp 2509-2514, 2007
23. Markovic Miroslav, Ragot Patrick, Perriard Yves, "Design optimization of a BLDC motor: a comparative analysis," IEEE Transactions, pp 1520-1523, 2007
24. Dailin Zhang, Youping Chen, Tom Kong Ching, Wu Ai, "Compensation scheme of position angle errors of permanent-magnet linear motors", IEEE Transactions on Magnetics, Vol 43, No. 10, pp 3868-3871, 2007
25. Tran H Thanh, Ha Quang, T. Nguyen Hung, "Robust non-overshoot time responses using cascade sliding mode-pid control", Journal of Advanced Computational Intelligence ,Vol.11,No.10, pp 1224-1225, 2007

26. Messner W, Bedillion M, Xia L, Karns D, “Lead and lag compensators with complex poles and zeros: design formulas for modeling and loop shaping.” IEEE Control Systems Magazine, Vol. 27, No. 1, pp. 44-54, 2007
27. Xin Xu Jian, “New lead compensator designs for control education and engineering”, Proceedings of the 27th Chinese Control Conference, pp 752-757, 2008
28. Ruderman Michael, Hoffmann Frank, Krettek Johannes, Torsten Bertram, “Detection and self-tuning compensation of periodic disturbances by the control of DC motor”, IEEE Transactions ,pp 1215-1220, 2008
29. Yeroglu Celaledin, Tan Nusret, “Development of a toolbox for frequency response analysis of fractional order control systems”, IEEE Transactions, pp 866-869, 2009
30. Dobra P, Dumitrache D, Tomesc L, Duma R, Trusca Mirela, “Low-cost embedded solution for PID controllers of DC motors”, IEEE Transactions, pp 1178-1183, 2009
31. Scott Jonathan, McLeish John, Round W Howell, “Speed control with low armature loss for very small sensorless brushed dc motors”, IEEE Transactions on Industrial Electronics, Vol. 56, No 4, pp 1223-1229, 2009
32. Srisertpol Jiraphon, Khajorntraidet Chanyut , “Estimation of dc motor variable torque using adaptive compensation”, IEEE Transactions, pp 712-717, 2009
33. Sang Qian, Tao Gang, “Gain margins of adaptive control systems”, IEEE Transactions, Vol. 55, No. 1, pp 104-115, 2010